## Materials and methods

### Chemicals and animals

Methimazole (2-mercapto-1-methylimidazole: MMI; CAS No. 60-56-0) was purchased from Sigma Chemical Co. (St. Louis, MO, USA). Pregnant Sprague–Dawley (SD) rats and adult male SD rats were obtained from Japan SLC, Inc. (Hamamatsu, Japan) at gestational day (GD) 1 (observation of vaginal plug was designated as GD 0) and postnatal day (PND) 35 (where PND 0 is the day of delivery), respectively. Animals were housed individually in polycarbonate cages with wood chip bedding, in an air-conditioned animal room maintained on a 12 h light–dark cycle at a temperature at 23 ± 2 °C with a relative humidity of 55 ± 15 %. Animals were allowed free access to food and water throughout the experimental period. A pelleted basal diet (MF-diet; Oriental Yeast Co., Ltd., Tokyo, Japan) and tap water were provided during the 10-day acclimatization period.

### Experimental design

Two experiments were carried out. In Experiment 1, MMI was administered to dams (developmental exposure). Twenty-four dams were randomly divided into three groups of eight dams each and treated with 0, 50, or 200 ppm of MMI in the drinking water from GD 10 to PND 21. Based on our previous studies that have shown apparent aberrations in neuronal development in the hippocampal structure in offspring (Shibutani et al. 2009; Saegusa et al. 2010), the highest dose in combination with the duration of MMI-treatment was determined as shown above. Each dam was housed with her litter individually, and body weights and food and water intakes were measured regularly. All litters were culled to 8 pups on PND 2, retaining the maximal number of males per litter. On PND 21, all dams and 3–4 male pups per litter were killed by exsanguination from the abdominal aorta under deep anesthesia with ether. The remaining animals were maintained until PND 77. From PND 21, all offspring consumed the basal diet and tap water. All pups were killed on PND 77.

In Experiment 2, male SD rats were randomly divided into three groups of ten animals each and treated with 0, 50, or 200 ppm MMI in the drinking water from PND 46 to PND 77 (adult-stage exposure). All animals were killed on PND 77 in the same way as Experiment 1.

All animal experiments were conducted in accordance with the "Guidelines for Proper Conduct of Animal Experiments" (Science Council of Japan, June 1, 2006) and the protocol was approved by the Animal Care and Use Committee of the Tokyo University of Agriculture and Technology.

### Thyroid-related hormone measurement

Before killing, blood samples were collected from the abdominal aorta under anesthesia from dams and male offspring in Experiment 1 and adult animals in Experiment 2. Plasma was prepared and stored at −30 °C. Concentrations of thyroid-stimulating hormone (TSH), triiodothyronine ($T_3$) and thyroxine ($T_4$) were measured by the chemiluminescent enzyme immunoassay method with the use of DPC Immulyze (Siemens Healthcare Diagnostics Inc., IL, USA).

### Histopathology, immunohistochemistry and apoptosis assays

For immunohistochemical analysis, brains of 10 male pups/group (1 or 2 pups/litter) at PND 21 and PND 77 in Experiment 1 and 10 animals/group in Experiment 2 were fixed in Bouin's solution overnight at room temperature. Coronal slices were routinely processed from brains of PND 21 and PND 77 at −3.0 and −3.5 mm from the bregma, respectively, for paraffin embedding.

Histopathological analysis was performed on the brain sections (3 μm in thickness) stained with hematoxylin and eosin.

Immunohistochemistry was performed on the brain sections (3 μm in thickness) with antibodies against proliferating cell nuclear antigen (PCNA; mouse monoclonal, clone PC10, 1:200, Dako, Glostrup, Denmark), paired box 6 (Pax6; mouse monoclonal, clone AD2.38, 1:500, Abcam Inc., Cambridge, UK), doublecortin (Dcx; rabbit polyclonal, 1:1,000, Abcam Inc.), parvalbumin (Pvalb; mouse monoclonal, 1:1,000, Millipore, Billerica, MA, USA), and calretinin (Calb2; mouse monoclonal, 1:100, LifeSpan Biosciences, Inc., Seattle, WA, USA). Antigen retrieval was applied for Pvalb and Calb2 antibodies by microwaving sections at 90 °C for 10 min in 10 mM citrate buffer (pH 6.0). No antigen retrieval was performed for the other antibodies. Immunodetection was carried out using a VECTASTAIN® Elite ABC kit (Vector Laboratories Inc., Burlingame, CA, USA) with 3,3′-diaminobenzidine/$H_2O_2$ as the chromogen. Sections were then counterstained with hematoxylin for microscopic examination.

In order to detect apoptosis, terminal deoxynucleotidyl transferase dUTP nick end labeling (TUNEL) was carried out using the ApopTag® Peroxidase In situ Apoptosis Detection kit (Millipore).

### Analysis of immunolocalization and apoptotic cells

PCNA-, Pax6-, Dcx-, or TUNEL-positive cells distributed in the SGZ of the dentate gyrus were counted bilaterally and the number was normalized with the length of the SGZ

(Fig. 1). In the dentate hilus, Pvalb- and Calb2-positive cells were counted bilaterally and the number was normalized with the hilus area. For quantitative measurement of each immunoreactive cell, digital photographs were taken with a 20× or 40× objective using a BX51 microscope (Olympus Optical Co., Ltd., Tokyo, Japan) attached to a DP70 Digital Camera System (Olympus Optical Co., Ltd.), and quantitative measurements were performed using the WinROOF image analysis software package (Version 5.7, Mitani Corp., Fukui, Japan).

## Real-time RT-PCR analysis

For real-time RT-PCR analysis, brains of 5 male pups/group in Experiment 1 at PND 21 and PND 77, and 6 males/group in Experiment 2 were fixed in methacarn solution for 6 h then dehydrated in 99.5 % ethanol at 4 °C overnight as described previously (Lee et al. 2006). Brains were coronally cut at the positions of +1 and −5 mm from the bregma. Cerebral cortical tissues were removed with tweezers, and whole hippocampi were dissected bilaterally. Dissected tissue samples were preserved in 99.5 % ethanol at −80 °C until analysis. Gene transcript levels for *Pax6* and *Dcx* in Experiment 1, and *Pvalb* and *Calb2* in both Experiment 1 and Experiment 2 were analyzed in the hippocampal tissues. Total RNA samples were extracted with the RNeasy Mini Kit (QIAGEN, Hilden, Germany), and first strand cDNA was synthesized using SuperScript™ III Reverse Transcriptase (Invitrogen Corp., Carlsbad, CA, USA). Then, real-time PCR analysis was performed using the Power SYBR® Green PCR Master Mix (Applied Biosystems Inc., Foster City, CA, USA) and the StepOnePlus™ Real-Time PCR System (Applied Biosystems Inc.). The PCR primers shown in Table 1 were designed using Primer Express software (Version 3.0; Applied Biosystems Inc.). Threshold cycle ($C_T$) values were first normalized to the housekeeping gene hypoxanthine guanine phosphoribosyltransferase (*Hprt*), as an endogenous control in the same sample, then used to calculate the relative differences in gene expression to a control $C_T$ value by the $2^{-\Delta\Delta C_T}$ method (Livak and Schmittgen 2001).

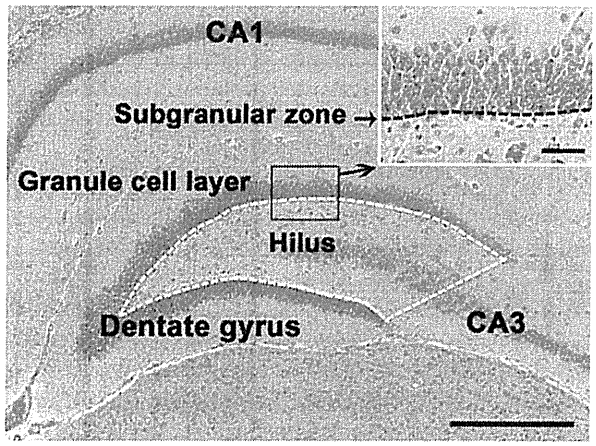


**Fig. 1** Overview of the hippocampal formation of a male rat at PND 21 stained with hematoxylin and eosin. *Inset* shows the granule cell layer and SGZ at higher magnification. Number of Pvalb and Calb2 immunoreactive cells in the hilus (enclosed by the *white dotted line*) was counted and normalized for the unit area. Number of immunoreactive cells for PCNA, Pax6, Dcx, and the number of TUNEL-positive cells in the SGZ (shown by a *black dotted line*) was counted and normalized for the unit length. Objective magnification, ×4 (*inset* ×40). *Bar* 500 μm (*inset* 50 μm)

## Statistical analysis

In Experiment 1, maternal data regarding the body and organ weights, food and water intake, and plasma concentrations of thyroid-related hormones were analyzed using the individual animal as the experimental unit. Offspring data regarding the body and organ weights were analyzed using the litter as the experimental unit. For data on thyroid-related hormone concentration, immunoreactive cell counts for each antigen or TUNEL-positive cells and real-time RT-PCR of pups, the individual animal was examined as the experimental unit. In Experiment 2, the individual animal was examined as the experimental unit for all data.

Differences in numerical data between the control and MMI-dosed groups in both Experiment 1 and 2 were evaluated in the following methods. First, the Bartlett's test

**Table 1** Sequence of primers used for real-time RT-PCR

| Gene | Accession no. | Forward primer (5′ → 3′) | Reverse primer (5′ → 3′) |
|---|---|---|---|
| *Pax6* | NM_013001 | GCCCTCACCAACACGTACAGT | GGTTATTTGCCATGGTGAAGCT |
| *Dcx* | NM_053379 | GGATTGTGTACGCTGTTTCTTCTG | TCAGGTCAGCCAGCAATGC |
| *Pvalb* | NM_022499 | TCGCCACAAAAAGTTCTTCCA | TCTTCACATCATCCGCACTCTT |
| *Calb2* | NM_053988 | AGCTCCAGGAGTACACCCAAAC | CCCAATTTGCCGTCTCCAT |
| *Hprt* | NM_012583 | GCCGACCGGTTCTGTCAT | TCATAACCTGGTTCATCATCACTAATC |

*Pax6* paired box 6, *Dcx* doublecortin, *Pvalb* parvalbumin, *Calb2* calretinin, *Hprt* hypoxanthine guanine phosphoribosyltransferase

was used for the homogeneity of variance between the groups. If the variance was homologous, Dunnett's test was performed for comparison between groups. If there was a significant difference in variance, Steel's test was used instead.

The incidences of histopathological lesions in the brain were statistically compared using the Fisher's exact probability test.

## Results

### Maternal parameters (Experiment 1)

In the study of developmental exposure, there was one animal that was non-pregnant in both the untreated control and 50 ppm groups, and one dam that was moribund at GD 21 in both the 50 and 200 ppm groups. Moribund dams did not show brooding behavior after delivery, and all of their pups died. Therefore, non-pregnant rats and moribund dams were excluded from the experiment. Throughout the gestation period, there were no statistically significant differences in body weight or food and water intake between the untreated control dams and MMI-treated dams at both doses, except for a significant and slight decrease of food intake at GD 20 (Online Resource 1, Fig. s1a, b, c). After delivery of offspring, food and water intakes were significantly lower in the MMI-treated dams at both doses than in the untreated controls, except for the unchanged values in food intake at 200 ppm on PND 18 and in water intake at 200 ppm on PND 2 and at 50 ppm and 200 ppm on PND 7 (Online Resource 1, Fig. s1b, c). The MMI intakes of dams from GD 10 to GD 20 were 5.59 mg/kg body weight/day for 50 ppm and 22.38 mg/kg body weight/day for 200 ppm. From PND 1 to PND 21, the intake values were 7.19 mg/kg body weight/day for 50 ppm and 26.43 mg/kg body weight/day for 200 ppm.

### Body weight, food intake and brain weight of offspring (Experiment 1)

Throughout the lactation period and after weaning to PND 77, body weights of the offspring in the MMI-exposed groups at both doses were significantly lower than the untreated control offspring (Online Resource 1, Fig. s2a). Food intake per animal was significantly lower in the 50 ppm MMI-exposed offspring after weaning (PND 21) to PND 35 and in the 200 ppm MMI-exposed offspring from PND 21 to PND 56 as compared with untreated control offspring (Online Resource 1, Fig. s2b). On PND 77, 200 ppm MMI-exposed offspring also showed significantly decreased food intake. On killing on PND 21, statistically significant decreases in the absolute brain weight and increases in relative brain weight were observed in MMI-exposed offspring at both doses (Online Resource 2, Table s1). A significant increase in relative brain weight was also observed in the 200 ppm MMI-exposed offspring at PND 77 (Online Resource 2, Table s1).

### Body weight, food and water intake, MMI intake and brain weight of animals receiving adult-stage MMI exposure (Experiment 2)

The body weights of animals treated with MMI decreased significantly from PND 60 to PND 77 at both doses (Online Resource 1, Fig. s3a). Food intake after PND 46 and water intake after PND 53 also decreased significantly in MMI-treated groups at both doses (Online Resource 1, Fig. s3b, c). On killing on PND 77, there were no significant differences in the absolute brain weight in MMI-treated groups at both doses, while the relative brain weight at both doses showed significant increases compared to the untreated controls (Online Resource 2, Table s1). Amount of MMI intakes during exposure period were 4.26 mg/kg body weight/day for 50 ppm and 16.00 mg/kg body weight/day for 200 ppm.

### Plasma levels of thyroid-related hormones

In the developmental exposure study (Experiment 1), statistically significant decreases of plasma $T_3$ and $T_4$ concentrations were evident in MMI-exposed offspring at both doses on PND 21 (Online Resource 2, Table s2). Plasma TSH concentration was significantly elevated in MMI-exposed offspring at both doses. At PND 77, no significant differences in thyroid-related hormones were observed between the untreated control offspring and MMI-exposed offspring at both doses.

In the adult-stage exposure study (Experiment 2), statistically significant decreases of plasma $T_3$ and $T_4$ concentrations and increase of TSH concentration were observed in MMI-exposed groups at both doses.

**Table 2** Incidence of subcortical band heterotopia in the corpus callosum in Experiment 1

| | MMI (ppm) | | |
|---|---|---|---|
| | 0 (cont) | 50 | 200 |
| No. of animals examined | 10 | 10 | 10 |
| PND 21 | 0 | 1 | 2 |
| PND 77 | 0 | 2 | 9** |

** Significantly different from the untreated controls by Fisher's exact probability test ($P < 0.01$)

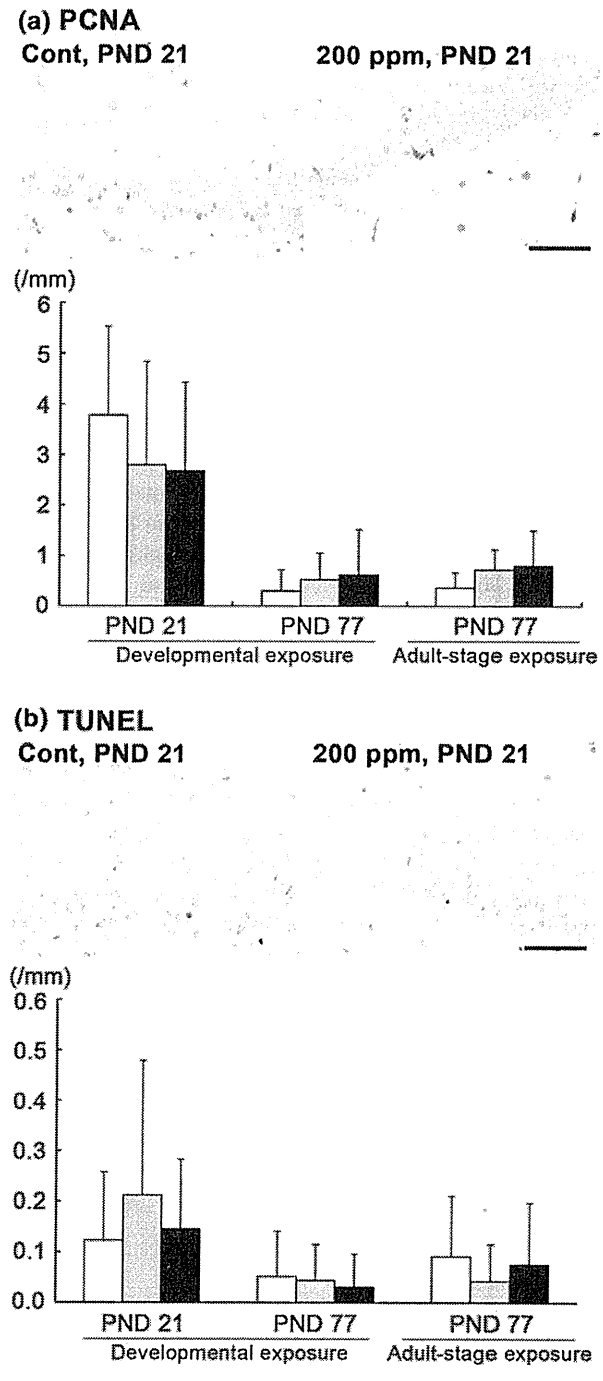


**Fig. 2** Distribution and number of positive cells for PCNA-▶ immunohistochemistry and TUNEL-assay in the SGZ of offspring at PND 21 and PND 77 in Experiment 1 and animals at PND 77 in Experiment 2. **a** PCNA-positive cells in the SGZ at PND 21 of an offspring of the untreated controls (*left*) and an offspring exposed to 200 ppm MMI (*right*) in Experiment 1. Objective magnification, ×40. *Bar* 50 μm. The graph shows the number of PCNA-positive cells/unit length (mm) of the SGZ in bilateral hemispheres. **b** TUNEL-positive cells in the SGZ at PND 21 of offspring of untreated controls (*left*) and offspring exposed to 200 ppm MMI (*right*) in Experiment 1. Objective magnification, ×40. *Bar* 50 μm. The graph shows the number of TUNEL-positive cells/unit length (mm) of the SGZ in bilateral hemispheres. *White column* untreated controls, *gray column* 50 ppm MMI, *black column* 200 ppm MMI. $N = 10$

### Histopathology of the brain

In the developmental exposure study (Experiment 1), subcortical band heterotopia was detected in the corpus callosum of MMI-exposed offspring at both doses on PND 21 and PND 77 (Table 2). Statistically significant increased incidence of this lesion was observed at 200 ppm on PND 77.

In the adult-stage exposure study (Experiment 2), development of subcortical band heterotopia was lacking by MMI-treatment.

### Proliferating and apoptotic cell counts in the SGZ

In the developmental exposure study (Experiment 1), there were no significant differences in the number of either PCNA-positive proliferating cells or TUNEL-positive apoptotic cells in the SGZ between the untreated control offspring and MMI-exposed offspring at both doses on PND 21 and PND 77 (Fig. 2a, b).

In the adult-stage exposure study (Experiment 2), there were no significant differences in the number of both PCNA-positive cells and TUNEL-positive cells between the untreated controls and MMI-treated animals at both doses (Fig. 2a, b).

### Neuronal progenitor cells in the SGZ

In the developmental exposure study (Experiment 1), statistically significant decreases in the number of Pax6-positive cells in the 200 ppm group and Dcx-positive cells in the 50 and 200 ppm groups were observed at PND 21 (Fig. 3a, b). At PND 77, the number of Pax6-positive cells was also significantly decreased in MMI-exposed offspring at both doses compared to the untreated control offspring, whereas there were no significant differences in the number of Dcx-positive cells in MMI-exposed offspring at both doses (Fig. 3a, b).

In the adult-stage exposure study (Experiment 2), no statistically significant changes in the number of Pax6- or Dcx-positive cells were observed between the untreated controls and MMI-treated animals at both doses (Fig. 3a, b).

### GABAergic interneurons in the dentate hilus

In the developmental exposure study (Experiment 1), statistically significant decreases in the number of Pvalb-positive cells and increases in Calb2-positive cells were observed in MMI-exposed offspring at both doses on PND

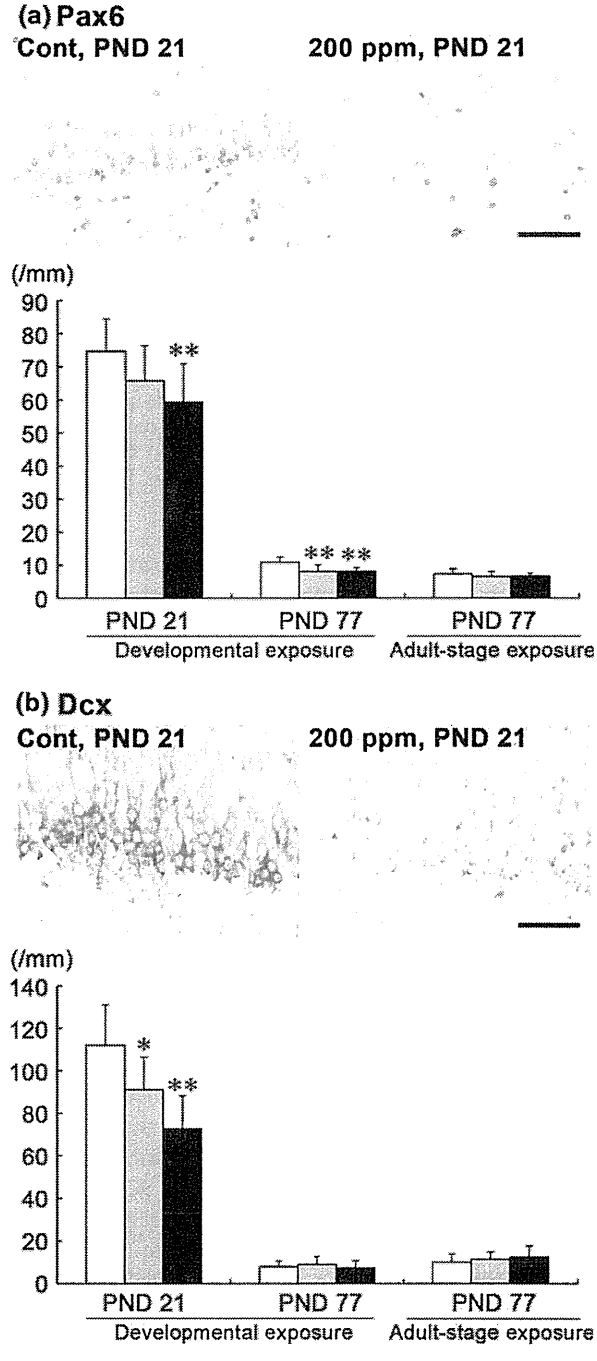


**Fig. 3** Distribution and number of Pax6- and Dcx-immunoreactive ▶ cells in the SGZ of the dentate gyrus. **a** Pax6-positive cells in the SGZ at PND 21 of an offspring of the untreated controls (*left*) and an offspring exposed to 200 ppm MMI (*right*) in Experiment 1. Note the lower number of Pax6-positive cells in the offspring exposed to 200 ppm MMI compared with the control offspring. Objective magnification, ×40. *Bar* 50 μm. The graph shows the number of Pax6-positive cell/unit length (mm) of the bilateral hemispheres of offspring at PND 21 and PND 77 in Experiment 1 and animals at PND 77 in Experiment 2. **b** Dcx-positive cells in the SGZ at PND 21 of offspring of untreated controls (*left*) and offspring exposed to 200 ppm MMI (*right*) in Experiment 1. Note the lower number of Dcx-positive cells in the offspring exposed to 200 ppm MMI as compared with the control offspring. Objective magnification, ×40. *Bar* 50 μm. The graph shows the number of Dcx-positive cell/unit length (mm) of bilateral hemispheres of offspring at PND 21 and PND 77 in Experiment 1 and animals at PND 77 in Experiment 2. *White column* untreated controls, *gray column* 50 ppm MMI, *black column* 200 ppm MMI. $N = 10$. *, **Significantly different from the corresponding control animals by Dunnett's or Steel's test ($P < 0.05$; $P < 0.01$)

21 (Fig. 4a, b). At PND 77, a similar change was observed in the 200 ppm MMI-exposed offspring (Fig. 4a, b).

In the adult-stage exposure study (Experiment 2), the number of Pvalb-positive cells significantly decreased in MMI-treated animals at both doses, while the number of Calb2-positive cells showed a significant increase in MMI-treated animals at both doses (Fig. 4a, b).

Real-time RT-PCR data

In the developmental exposure study (Experiment 1), there were no statistically significant fluctuations in *Pax6* and *Dcx* mRNA levels between the untreated control offspring and MMI-exposed offspring at both doses on both PND 21 and PND 77 (Fig. 5a, b). However, the level of *Pvalb* mRNA significantly decreased at 200 ppm in MMI-exposed offspring on both PND 21 and PND 77 (Fig. 5a, b). There was a significant increase in transcript level of *Calb2* in 200 ppm MMI-exposed offspring at PND 21, whereas no significant difference was observed at PND 77 (Fig. 5a, b).

In the adult-stage exposure study (Experiment 2), mRNA levels of both *Pvalb* and *Calb2* showed no significant differences between the untreated controls and MMI-treated animals at both doses (Fig. 5c).

## Discussion

In the present study, developmental hypothyroidism caused by maternal exposure to MMI induced subcortical band heterotopia in the corpus callosum as a result of aberrant neuronal migration due to TH insufficiency in offspring (Goodman and Gilbert 2007; Shibutani et al. 2009). In the SGZ, the number of Pax6-positive cells, one of the markers of early neuronal progenitors, decreased at both PND 21 and PND 77, while no apparent effect was observed in proliferation and apoptosis of progenitor cells at PND 21. A decrease in Dcx-positive cells was also observed at PND 21. In the dentate hilus, developmental hypothyroidism caused a decrease in Pvalb-positive cell number and an increase in Calb2-positive cells; at the high dose this increase was sustained into the adult stage. In contrast,

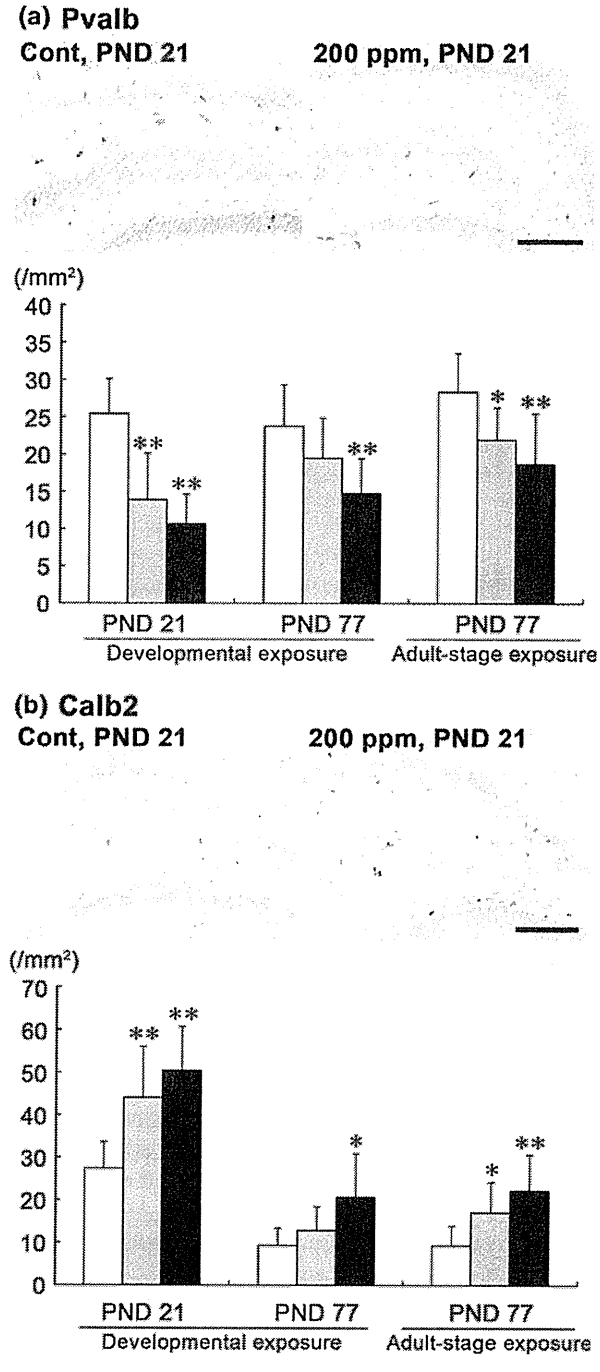


**Fig. 4** Distribution and number of Pvalb- and Calb2-immunoreactive cells in the hilus of the dentate gyrus. **a** Pvalb-positive cells in the hilus of an offspring of untreated controls (*left*) at PND 21 and an offspring exposed to 200 ppm MMI (*right*) at PND 21 in Experiment 1. Note the lower number of Pvalb-positive cells in the offspring exposed to 200 ppm MMI as compared with the control offspring. Objective magnification, ×10. *Bar* 200 μm. The graph shows the number of Pvalb-positive cell/unit area ($mm^2$) of the bilateral hemispheres of offspring at PND 21 and PND 77 in Experiment 1 and animals at PND 77 in Experiment 2. **b** Calb2-positive cells in the hilus at PND 21 of offspring of untreated controls (*left*) and offspring exposed to 200 ppm MMI (*right*) in Experiment 1. Note the higher number of Calb2-positive cells in the offspring exposed to 200 ppm MMI as compared with the control offspring. Objective magnification, ×10. *Bar* 200 μm. The graph shows the number of Calb2-positive cell/unit area ($mm^2$) of the bilateral hemispheres of offspring at PND 21 and PND 77 in Experiment 1 and animals at PND 77 in Experiment 2. *White column* untreated controls, *gray column* 50 ppm MMI, *black column* 200 ppm MMI. $N = 10$. *, **Significantly different from the corresponding control animals by Dunnett's or Steel's test ($P < 0.05$; $P < 0.01$)

adult-stage hypothyroidism did not induce subcortical band heterotopia in the corpus callosum. There also were no changes in proliferation, apoptosis, or differentiation of progenitor cells in the SGZ, while interneuron populations in the hilus fluctuated similar to developmental hypothyroidism. To our knowledge, the present study was the first to show these interneuron population changes in adult-stage hypothyroidism (Wallis et al. 2008). Thus, even with adult-stage hypothyroidism, we found fluctuations in the number of interneurons similar to those observed in developmental hypothyroidism, while we did not detect any changes in neurogenesis.

It is well known that developmental hypothyroidism typically targets hippocampal neurogenesis in rats, causing impairment of granule cell maturation in the SGZ and irreversible reduction of the total number of granule cells in the dentate gyrus (Gong et al. 2010; Koromilas et al. 2010). In the present study, offspring at PND 21 after developmental hypothyroidism showed a sustained reduction of Pax6-positive cells, which represent type-1 stem cells and type-2a early stage progenitor cells in the SGZ, and a reduction of Dcx-positive cells, which represent the cell population from type-2b progenitor cells to immature granule cells in the SGZ. We also found thinning of the granule cell layer at both PND 21 and PND 77 in the present study (data not shown). These results may suggest that developmental hypothyroidism affects neuronal differentiation of newly generated earlier-stage progenitor cells in the SGZ, resulting in the reduction of mature granular cells. There may be a close relation between the affection of progenitor cell differentiation observed here and hypothyroidism-induced neuronal mismigration (Lavado-Autric et al. 2003; Shibutani et al. 2009). However, different from apparent effect on cell proliferation of progenitor cells by PTU-induced developmental hypothyroidism in our previous study (Saegusa et al. 2010), the effect of MMI-induced hypothyroidism on cell proliferation in the SGZ in the present study may be mild, because nascent cell proliferation activity as estimated by PCNA immunoreactivity was unchanged between euthyroid and hypothyroid cases at PND 21.

Because hypothyroidism targets stem cells and earlier progenitor cells as revealed in the present study, effect of

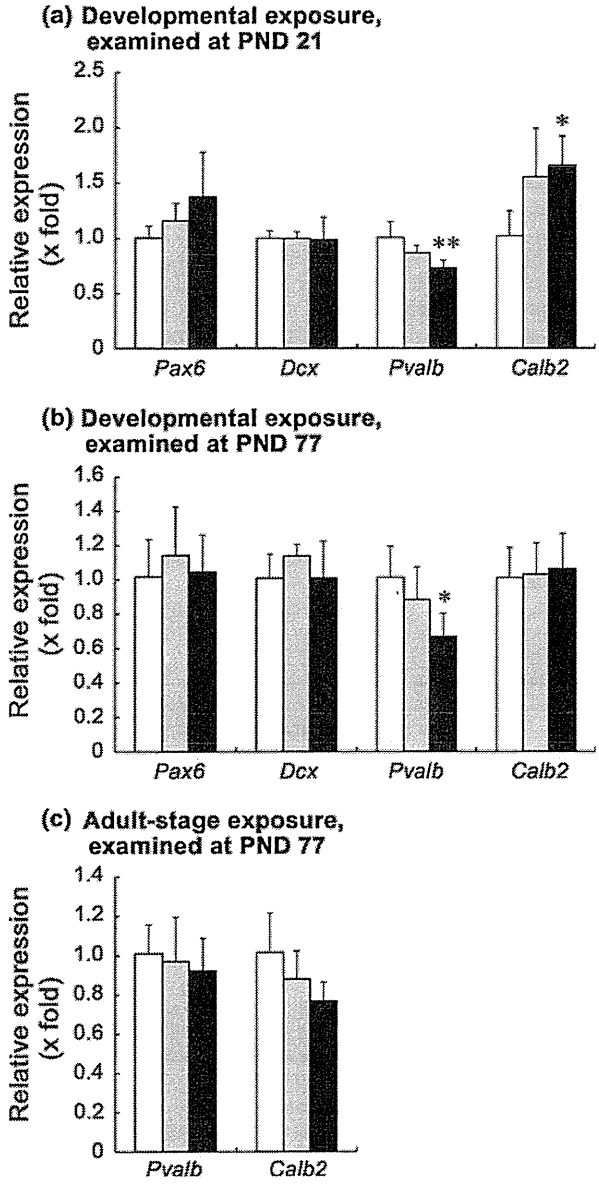


**Fig. 5** The relative mRNA expression in the hippocampal tissue analyzed by real-time RT-PCR. **a** *Pax6*, *Dcx*, *Pvalb*, and *Calb2* in offspring at PND 21 in Experiment 1. **b** *Pax6*, *Dcx*, *Pvalb*, and *Calb2* of offspring at PND 77 in Experiment 1. **c** *Pvalb*, and *Calb2* in animals at PND 77 in Experiment 2. *White column* untreated controls, *gray column* 50 ppm MMI, *black column* 200 ppm MMI. $N = 5$ (Experiment 1), and 6 (Experiment 2). *, **Significantly different from the corresponding control animals by Dunnett's or Steel's test ($P < 0.05$; $P < 0.01$)

hypothyroidism on neurogenesis could be dependent on the activity of neurogenesis. Several studies have shown changes in adult neurogenesis in the hippocampal SGZ in rats with adult-stage hypothyroidism, such as decreases in newborn cell survival and differentiation (Ambrogini et al. 2005; Desouza et al. 2005; Zhang et al. 2009). However, these studies labeled progenitor cells by consecutive injections or continuous infusion of 5-bromo-2′-deoxyuridine, which may reflect a mild turnover of granule cells at the adult stage. Therefore, the impact of adult-stage hypothyroidism on adult neurogenesis in the present study may be so small that it cannot be detected by phenotype analysis using the neuronal stage-defining markers examined here.

A reduction in the number of Pvalb-positive cells and the GABAergic terminals was reported in TH receptor α1 (TRα1) mutant mice (Venero et al. 2005). Also, lack of $T_3$ during early development led to irreversible defects in the maturation of GABAergic systems, and Pvalb-positive interneurons especially showed delayed or incomplete maturation (Berbel et al. 1996; Gilbert et al. 2007; Wallis et al. 2008). Therefore, decreases in Pvalb-positive cells observed in both of the developmental and adult-stage hypothyroidism in the present study may be a reflection of reduced TH stimuli. In addition to inhibiting hippocampal granule cells, GABAergic interneurons play an important role in adult hippocampal neurogenesis (Duveau et al. 2011; Masiulis et al. 2011; Kapoor et al. 2011). Particularly, GABAergic interneurons provide direct neural inputs to type-2 progenitor cells in the SGZ and promote neural differentiation (Tozuka et al. 2005). Moreover, progenitor cell proliferation is promoted by the GABAergic system (Yoo et al. 2011). Therefore, in the present study, reduction of Pvalb-positive cells may lead to a decrease in GABAergic input onto SGZ progenitor cells, affecting neurogenesis even at the adult stage. However, we could detect changes in adult neurogenesis only after developmental hypothyroidism.

Pvalb-positive cells are known to have high average activity level and are considered to play a central role in inhibition of granule cells activity (Gulyás et al. 2006). A decrease in Pvalb-positive cells during development causes suppression of GABA-mediated granule cell inhibition (Gilbert et al. 2007). Moreover, TRα1 mutant mice showed anxiety, one of the symptoms recognized in both ADHD and anxiety syndrome in humans, as well as a decrease in the number of Pvalb-positive cells and GABAergic terminals (Venero et al. 2005). Therefore, the significantly decreased population of Pvalb-positive cells in both developmental and adult onset hypothyroidism in the present study may lead to symptoms of both ADHD and anxiety.

In the present study, an increase in the number of Calb2-positive cells was also observed in both developmental and adult-stage hypothyroidism. Of the several subtypes of GABAergic interneurons in the hippocampus, Calb2-positive interneurons are known to interconnect interneurons in the dentate gyrus and may coordinate the activity of the entire hippocampus by controlling the activity of inhibitory

neurons connecting to granule cells (Gulyás et al. 1996). Hence, the increase in Calb2-positive cells is considered to be secondary to the decrease in number of Pvalb-positive cells.

In conclusion, we found fluctuations in GABAergic interneuron subpopulations in both developmental and adult-stage hypothyroidism. While developmental hypothyroidism resulted in continued impairment of neurogenesis, we could not detect any apparent changes in neurogenesis in adult-stage hypothyroidism. Considering their role in neurogenesis, changes in GABAergic interneuron subpopulations may provide a sensitive tool for detection of aberrant neurogenesis. Our study also suggests that analysis of interneuron subpopulations may provide a tool for detection of changes in neurogenesis, particularly for regular toxicity tests such as the 28-day repeated-oral dose-toxicity test.

**Acknowledgments** The authors thank Mrs. Shigeko Suzuki for her technical assistance in preparing the histological specimens. This work was supported by a grant from Ministry of Economy, Trade and Industry (METI), Japan.

**Conflict of interest** All authors disclose that there are no conflicts of interest that could inappropriately influence the outcome of the present study.

## References

Akaike M, Kato N, Ohno H, Kobayashi T (1991) Hyperactivity and spatial maze learning impairment of adult rats with temporary neonatal hypothyroidism. Neurotoxicol Teratol 13:317–322

Almeida C, Brasil MA, Costa AJ, Reis FA, Reuters V, Teixeira P, Ferreira M, Marques AM, Melo BA, Teixeira LB, Buescu A, Vaisman M (2007) Subclinical hypothyroidism: psychiatric disorders and symptoms. Rev Bras Psiquiatr 29:157–159

Ambrogini P, Cuppini R, Ferri P, Mancini C, Ciaroni S, Voci A, Gerdoni E, Gallo G (2005) Thyroid hormones affect neurogenesis in the dentate gyrus of adult rat. Neuroendocrinology 81:244–253

Berbel P, Marco P, Cerezo JR, DeFelipe J (1996) Distribution of parvalbumin immunoreactivity in the neocortex of hypothyroid adult rats. Neurosci Lett 204:65–68

Bernal J, Nunez J (1995) Thyroid hormones and brain development. Eur J Endocrinol 133:390–398

Breunig JJ, Silbereis J, Vaccarino FM, Sestan N, Rakic P (2007) Notch regulates cell fate and dendrite morphology of newborn neurons in the postnatal dentate gyrus. Proc Natl Acad Sci USA 104:20558–20563

Choi JH, Yoo KY, Lee CH, Yi SS, Yoo DY, Seong JK, Yoon YS, Hwang IK, Won MH (2011) Effects of treadmill exercise combined with MK 801 treatment on neuroblast differentiation in the dentate gyrus in rats. Cell Mol Neurobiol 31:285–292

Delange F (2000) The role of iodine in brain development. Proc Nutr Soc 59:75–79

Desouza LA, Ladiwala U, Daniel SM, Agashe S, Vaidya RA, Vaidya VA (2005) Thyroid hormone regulates hippocampal neurogenesis in the adult rat brain. Mol Cell Neurosci 29:414–426

Duveau V, Laustela S, Barth L, Gianolini F, Vogt KE, Keist R, Chandra D, Homanics GE, Rudolph U, Fritschy JM (2011) Spatiotemporal specificity of GABAA receptor-mediated regulation of adult hippocampal neurogenesis. Eur J Neurosci 34:362–373

Eriksson PS, Perfilieva E, Björk-Eriksson T, Alborn AM, Nordborg C, Peterson DA, Gage FH (1998) Neurogenesis in the adult human hippocampus. Nat Med 4:1313–1317

Gilbert ME, Sui L, Walker MJ, Anderson W, Thomas S, Smoller SN, Schon JP, Phani S, Goodman JH (2007) Thyroid hormone insufficiency during brain development reduces parvalbumin immunoreactivity and inhibitory function in the hippocampus. Endocrinology 148:92–102

Gong J, Liu W, Dong J, Wang Y, Xu H, Wei W, Zhong J, Xi Q, Chen J (2010) Developmental iodine deficiency and hypothyroidism impair neural development in rat hippocampus: involvement of doublecortin and NCAM-180. BMC Neurosci 11:50

Goodman JH, Gilbert ME (2007) Modest thyroid hormone insufficiency during development induces a cellular malformation in the corpus callosum: a model of cortical dysplasia. Endocrinology 148:2593–2597

Gulyás AI, Hájos N, Freund TF (1996) Interneurons containing calretinin are specialized to control other interneurons in the rat hippocampus. J Neurosci 16:3397–3411

Gulyás AI, Buzsáki G, Freund TF, Hirase H (2006) Populations of hippocampal inhibitory neurons express different levels of cytochrome c. Eur J Neurosci 23:2581–2594

Hodge RD, Kowalczyk TD, Wolf SA, Encinas JM, Rippey C, Enikolopov G, Kempermann G, Hevner RF (2008) Intermediate progenitors in adult hippocampal neurogenesis: Tbr2 expression and coordinate regulation of neuronal output. J Neurosci 28:3707–3717

Houser CR (2007) Interneurons of the dentate gyrus: an overview of cell types, terminal fields and neurochemical identity. Prog Brain Res 163:217–232

Hwang IK, Yoo KY, Yoo DY, Choi JH, Lee CH, Kang IJ, Kwon DY, Kim YS, Kim DW, Won MH (2011) Zizyphus enhances cell proliferation and neuroblast differentiation in the subgranular zone of the dentate gyrus in middle-aged mice. J Med Food 14:195–200

Kapoor R, Ghosh H, Nordstrom K, Vennstrom B, Vaidya VA (2011) Loss of thyroid hormone receptor $\beta$ is associated with increased progenitor proliferation and NeuroD positive cell number in the adult hippocampus. Neurosci Lett 487:199–203

Knoth R, Singec I, Ditter M, Pantazis G, Capetian P, Meyer RP, Horvat V, Volk B, Kempermann G (2010) Murine features of neurogenesis in the human hippocampus across the lifespan from 0 to 100 years. PLoS ONE 5:e8809

Koromilas C, Liapi C, Schulpis KH, Kalafatakis K, Zarros A, Tsakiris S (2010) Structural and functional alterations in the hippocampus due to hypothyroidism. Metab Brain Dis 25:339–354

Lee KY, Shibutani M, Inoue K, Kuroiwa K, U M, Woo GH, Hirose M (2006) Methacarn fixation—effects of tissue processing and storage conditions on detection of mRNAs and proteins in paraffin-embedded tissues. Anal Biochem 351:36–43

Lavado-Autric R, Ausó E, García-Velasco JV, Arufe Mdel C, Escobar del Rey F, Berbel P, Morreale de Escobar G (2003) Early maternal hypothyroxinemia alters histogenesis and cerebral cortex cytoarchitecture of the progeny. J Clin Invest 111:1073–1082

Livak KJ, Schmittgen TD (2001) Analysis of relative gene expression data using real-time quantitative PCR and the $2^{-\Delta\Delta C_T}$ method. Methods 25:402–408

Masiulis I, Yun S, Eisch AJ (2011) The interesting interplay between interneurons and adult hippocampal neurogenesis. Mol Neurobiol. doi:10.1007/s12035-011-8207-z

Montero-Pedrazuela A, Venero C, Lavado-Autric R, Fernández-Lamo I, García-Verdugo JM, Bernal J, Guadaño-Ferraz A (2006) Modulation of adult hippocampal neurogenesis by thyroid hormones: implications in depressive-like behavior. Mol Psychiatry 11:361–371

Nam SM, Yoo DY, Kim W, Yoo M, Kim DW, Won MH, Hwang IK, Yoon YS (2011) Effects of s-allyl-L-cysteine on cell proliferation and neuroblast differentiation in the mouse dentate gyrus. J Vet Med Sci 73:1071–1075

Negishi T, Kawasaki K, Sekiguchi S, Ishii Y, Kyuwa S, Kuroda Y, Yoshikawa Y (2005) Attention-deficit and hyperactive neurobehavioural characteristics induced by perinatal hypothyroidism in rats. Behav Brain Res 159:323–331

Pineda-Reynoso M, Cano-Europa E, Blas-Valdivia V, Hernandez-Garcia A, Franco-Colin M, Ortiz-Butron R (2010) Hypothyroidism during neonatal and perinatal period induced by thyroidectomy of the mother causes depressive-like behavior in prepubertal rats. Neuropsychiatr Dis Treat 6:137–143

Saegusa Y, Woo GH, Fujimoto H, Kemmochi S, Shimamoto K, Hirose M, Mitsumori K, Nishikawa A, Shibutani M (2010) Sustained production of Reelin-expressing interneurons in the hippocampal dentate hilus after developmental exposure to antithyroid agents in rats. Reprod Toxicol 29:407–414

Sait Gönen M, Kisakol G, Savas Cilli A, Dikbas O, Gungor K, Inal A, Kaya A (2004) Assessment of anxiety in subclinical thyroid disorders. Endocr J 51:311–315

Schoonover CM, Seibel MM, Jolson DM, Stack MJ, Rahman RJ, Jones SA, Mariash CN, Anderson GW (2004) Thyroid hormone regulates oligodendrocyte accumulation in developing rat brain white matter tracts. Endocrinology 145:5013–5020

Shibutani M, Woo GH, Fujimoto H, Saegusa Y, Takahashi M, Inoue K, Hirose M, Nishikawa A (2009) Assessment of developmental effects of hypothyroidism in rats from in utero and lactation exposure to anti-thyroid agents. Reprod Toxicol 28:297–307

Tozuka Y, Fukuda S, Namba T, Seki T, Hisatsune T (2005) GABAergic excitation promotes neuronal differentiation in adult hippocampal progenitor cells. Neuron 47:803–815

Venero C, Guadaño-Ferraz A, Herrero AI, Nordström K, Manzano J, de Escobar GM, Bernal J, Vennström B (2005) Anxiety, memory impairment, and locomotor dysfunction caused by a mutant thyroid hormone receptor α1 can be ameliorated by $T_3$ treatment. Genes Dev 19:2152–2163

Vermiglio F, Lo Presti VP, Moleti M, Sidoti M, Tortorella G, Scaffidi G, Castagna MG, Mattina F, Violi MA, Crisà A, Artemisia A, Trimarchi F (2004) Attention deficit and hyperactivity disorders in the offspring of mothers exposed to mild-moderate iodine deficiency: a possible novel iodine deficiency disorder in developed countries. J Clin Endocrinol Metab 89:6054–6060

Wallis K, Sjögren M, van Hogerlinden M, Silberberg G, Fisahn A, Nordström K, Larsson L, Westerblad H, Morreale de Escobar G, Shupliakov O, Vennström B (2008) Locomotor deficiencies and aberrant development of subtype-specific GABAergic interneurons caused by an unliganded thyroid hormone receptor α1. J Neurosci 28:1904–1915

Yan BC, Yoo KY, Park JH, Lee CH, Choi JH, Won MH (2011) The high dosage of earthworm (*Eisenia andrei*) extract decreases cell proliferation and neuroblast differentiation in the mouse hippocampal dentate gyrus. Anat Cell Biol 44:218–225

Yoo DY, Kim W, Kim DW, Yoo KY, Chung JY, Youn HY, Yoon YS, Choi SY, Won MH, Hwang IK (2011) Pyridoxine enhances cell proliferation and neuroblast differentiation by upregulating the GABAergic system in the mouse dentate gyrus. Neurochem Res 36:713–721

Zhang L, Blomgren K, Kuhn HG, Cooper-Kuhn CM (2009) Effects of postnatal thyroid hormone deficiency on neurogenesis in the juvenile and adult rat. Neurobiol Dis 34:366–374

Reproductive Toxicology xxx (2012) xxx–xxx

Contents lists available at SciVerse ScienceDirect

Reproductive Toxicology

journal homepage: www.elsevier.com/locate/reprotox

# Increased cellular distribution of vimentin and Ret in the cingulum induced by developmental hypothyroidism in rat offspring maternally exposed to anti-thyroid agents

Hitoshi Fujimoto[a], Gye-Hyeong Woo[a], Kaoru Inoue[a], Katsuhide Igarashi[b], Jun Kanno[b], Masao Hirose[c], Akiyoshi Nishikawa[d], Makoto Shibutani[a,e,*]

[a] Division of Pathology, National Institute of Health Sciences, 1–18–1 Kamiyoga, Setagaya-ku, Tokyo 158-8501, Japan
[b] Division of Molecular Toxicology, National Institute of Health Sciences, 1–18–1 Kamiyoga, Setagaya-ku, Tokyo 158-8501, Japan
[d] Biological Safety Research Center, National Institute of Health Sciences, 1–18–1 Kamiyoga, Setagaya-ku, Tokyo 158-8501, Japan
[c] Food Safety Commission, 5–2–20 Akasaka Park Bld. 22nd Floor, Akasaka, Minato-ku, Tokyo 107-6122, Japan
[e] Laboratory of Veterinary Pathology, Tokyo University of Agriculture and Technology, 3–5–8 Saiwai-cho, Fuchu-shi, Tokyo 183-8509, Japan

ARTICLE INFO

*Article history:*
Received 4 December 2011
Received in revised form 19 February 2012
Accepted 16 March 2012
Available online xxx

*Keywords:*
Developmental hypothyroidism
Cerebral white matter
Vimentin
Ret
Rat

ABSTRACT

To elucidate target molecules of white matter development responding to hypothyroidism, global gene expression profiling of cerebral white matter from male rat offspring was performed after maternal exposure to anti-thyroid agents, 6-propyl-2-thiouracil and methimazole, on postnatal day 20. Genes involved in central nervous system development commonly up- or down-regulated among groups treated with anti-thyroid agents. Immunohistochemical distributions of vimentin, Ret proto-oncogene (Ret), deleted in colorectal cancer protein (DCC), and Claudin11 (Cld11) were examined based on the gene expression profile. Immunoreactive cells for vimentin and Ret in the cingulum, and the immunoreactive intensity of Cld11 and DCC in whole white matter were increased by treatment with anti-thyroid agents. Immunoreactive cells for vimentin and Ret were immature astrocytes and oligodendrocytes, respectively. Thus, immunoreactive cells for vimentin and Ret may be quantitatively measurable targets of developmental hypothyroidism in white matter.



## 1. Introduction

Thyroid hormones are essential for normal fetal and neonatal brain development, control neuronal and glial proliferation in definitive brain regions and regulate neuronal migration and differentiation [1–3]. In humans, maternal hypothyroxinemia early in pregnancy may adversely affect fetal brain development, and importantly, even mild to moderate hypothyroxinemia may result in suboptimal neurodevelopment [4], thereby increasing the concern of impaired brain development induced by exposure to thyroid hormone-disrupting chemicals in the environment.

Developmental hypothyroidism leads to growth retardation, neurological defects and impaired performance in various behavioral learning actions [5,6]. Rat offspring maternally exposed to anti-thyroid agents, such as 6-propyl-2-thiouracil (PTU) and methimazole (MMI), show impaired brain growth including white matter hypoplasia with decreased axonal myelination and oligodendrocytes, and impairment of neurogenesis, neuronal migration, dendritic arborization and synapse formation [2,7–9]. These types of impaired brain growth are permanent and accompanied by apparent structural and functional abnormalities. However, the molecular mechanism of impaired brain growth is still unclear.

Histological lesion-specific gene expression profiling provides valuable information on the mechanisms underlying lesion development. In previous studies, we established molecular analysis methods for DNA, RNA and proteins in paraffin-embedded small tissue specimens using the organic solvent-based fixative methacarn, with high performance similar to that of unfixed frozen tissue specimens [10–12]. These methods have been used to analyze global gene expression changes in microdissected lesions [13–15].

*Abbreviations:* CC, corpus callosum; Cld11, claudin 11; CNS, central nervous system; DCC, deleted in colorectal cancer protein; GAPDH, glyceraldehyde 3-phosphate dehydrogenase; GD, gestation day; GDNF, glial cell line-derived neurotrophic factor; GFAP, glial fibrillary acidic protein; MMI, methimazole; OSP, oligodendrocyte specific protein; PCR, polymerase chain reaction; PND, postnatal day; PTU, 6-propyl-2-thiouracil; Ret, Ret proto-oncogene; RT, reverse transcription; v-Maf, v-maf musculoaponeurotic fibrosarcoma oncogene; Zfhx1b, zinc finger homeobox 1b.

* Corresponding author at: Laboratory of Veterinary Pathology, Tokyo University of Agriculture and Technology, 3–5–8 Saiwai-cho, Fuchu-shi, Tokyo 183-8509, Japan. Tel.: +81 42 367 5874; fax: +81 42 367 5771.
*E-mail address:* mshibuta@cc.tuat.ac.jp (M. Shibutani).

0890-6238/$ – see front matter © 2012 Elsevier Inc. All rights reserved.
http://dx.doi.org/10.1016/j.reprotox.2012.03.005

To evaluate in vivo developmental brain growth effects of thyroid hormone-disrupting chemicals, we morphometrically analyzed neuronal migration and white matter development in a rat developmental hypothyroidism model [16]. Molecules involved in aberrant neurogenesis and neuronal mismigration were identified by global gene expression analysis of the hippocampal area [15]. In the present study, to elucidate marker molecules in white matter involved in developmental hypothyroidism, we performed global gene expression profiling using microarrays. To obtain the white matter-specific gene expression profile, a microdissection technique was applied to the corpus callosum (CC) and bilateral cerebral white matter. Based on expression profiles, cellular localization of selected molecules was then immunohistochemically examined in cerebral white matter after developmental exposure to anti-thyroid agents.

## 2. Materials and methods

### 2.1. Chemicals and animals

6-propyl-2-thiouracil (PTU; CAS No. 51-52-9) and methimazole (MMI; CAS No. 60-56-0) were purchased from Sigma Chemical Co. (St. Louis, MO). Pregnant CD® (SD) IGS rats at gestational day (GD) 3 (GD 0: the day vaginal plugs appeared) were purchased from Charles River Japan Inc. (Yokohama, Japan). Animals were individually housed in polycarbonate cages (SK-Clean, 41.5 cm × 26 cm × 17.5 cm; CLEA Japan Inc., Tokyo, Japan) with wood chip bedding (Sankyo Lab Service Corp., Tokyo, Japan) and maintained in a climate-controlled animal room (24 ± 1 °C, relative humidity: 55 ± 5%) with a 12 h light/dark cycle. A soy-free diet (Oriental Yeast Co. Ltd., Tokyo, Japan) was chosen as the basal diet for maternal animals to eliminate possible phytoestrogen effects [17]. Animals received food and water ad libitum throughout experimentation including a 1 week acclimation period.

### 2.2. Experimental design

Animal experiments are described elsewhere [16]. Briefly, maternal animals were randomly divided into four groups including an untreated control. Eight dams per group were treated with 3 or 12 ppm PTU or 200 ppm MMI, which was added to drinking water from GD 10 to postnatal day (PND) 20 (PND 0: the day of delivery). On PND 2, four male and four female offspring per dam were randomly selected and remaining litters were culled. On PND 20, 20 male and 20 female offspring (at least one male and one female per dam) per group were subjected to prepubertal necropsy [16,18]. All animals were weighed and sacrificed by exsanguination from the abdominal aorta under deep anesthesia with ether. Animal protocols were reviewed and approved by the Animal Care and Use Committee of the National Institute of Health Sciences, Japan.

### 2.3. Preparation of tissue specimens and microdissection

For microarray and real-time reverse transcription (RT)-polymerase chain reaction (PCR) analyses, the whole brain of male offspring was immediately removed at prepubertal necropsy on PND 20 ($n$ = 4/group) and fixed with methacarn solution for 2 h at 4 °C [10]. Coronal brain slices taken at −3.5 mm from the bregma were dehydrated and embedded in paraffin. Embedded tissues were stored at 4 °C until tissue sectioning for microdissection [19].

For microdissection, 4 and 20 μm-thick serial sections were prepared. The 4 μm-thick sections were stained with hematoxylin and eosin for confirmation of anatomical orientation of the hippocampal substructure to aid microdissection (Fig. 1). The 20 μm-thick sections were mounted onto PEN-foil film (Leica Microsystems GmbH, Welzlar, Germany) overlaid on glass slides, dried in an incubator overnight at 37 °C, and then stained using an LCM staining kit (Ambion, Inc., Austin, TX). Regions of CC and bilateral cerebral white matter (external capsule) in sections, as shown in Fig. 1, were subjected to laser microbeam microdissection (Leica Microsystems GmbH). Forty sections from each animal were used for microdissection, and microdissected samples were individually stored in 1.5 ml tubes at −80 °C until total RNA extraction.

### 2.4. RNA preparation, amplification and microarray analysis

Total RNA extraction from microdissected regions, quantitation of RNA yield, and RNA amplification were performed using methods described elsewhere [14,15,19].

For microarray analysis, second-round-amplified biotin-labeled antisense RNAs were subjected to hybridization with a GeneChip® Rat Genome 230 2.0 Array (Affymetrix, Inc., Santa Clara, CA).

Gene selection and normalization of expression data were performed using GeneSpring® software 7.2 (Silicon Genetics, Redwood City, CA). Per chip normalization was performed according to a method described elsewhere [14,15]. Genes with expression changes of at least 2-fold in magnitude compared with those of untreated controls were selected. Common genes with altered expression in anti-thyroid agent exposed groups were also selected.

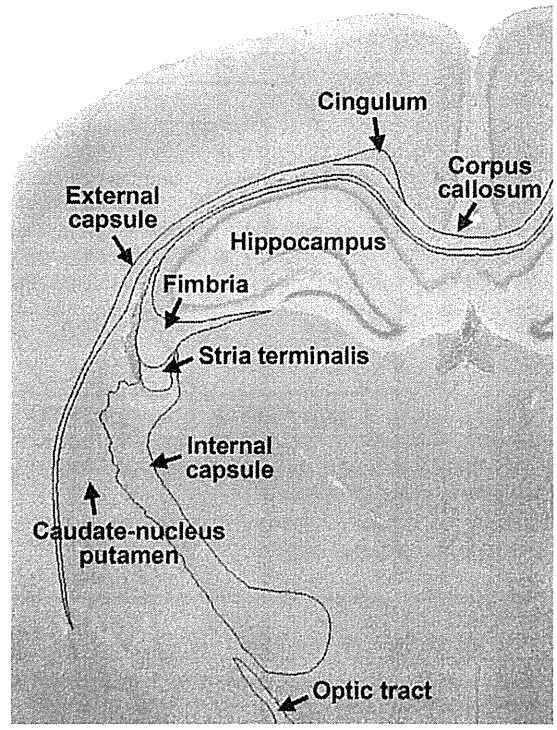


**Fig. 1.** Overview of the cerebral hemisphere of a male rat at PND 20 stained with hematoxylin and eosin. Magnification, 12.5×.

### 2.5. Real-time RT-PCR

Quantitative real-time RT-PCR using an ABI Prism 7900HT (Applied Biosystems Japan Ltd., Tokyo, Japan) was performed for confirmation of expression values obtained from microarray analysis. Selected genes showed altered expression (≥2-fold, ≤0.5-fold) in any of the anti-thyroid agent-exposed animals as compared with those of untreated controls. For example, vimentin, *Ret*, v-maf musculoaponeurotic fibrosarcoma oncogene (*v-Maf*) and tektin 4 as up-regulated genes, and *Cld11* and zinc finger homeobox 1b (*Zfhx1b*) as down-regulated ones. RT was performed using first-round antisense RNAs prepared for microarray analysis. For real-time PCR analysis, ABI Assays-on-Demand™ TaqMan® probe and primer sets from Applied Biosystems ($n$ = 4/group) were used. For quantification of expression data, a standard curve method was applied. Expression values were normalized to glyceraldehyde 3-phosphate dehydrogenase (GAPDH) using TaqMan® Rodent GAPDH Control Reagents (Applied Biosystems Japan Ltd.).

### 2.6. Immunohistochemistry

To evaluate the immunohistochemical distribution of molecules identified by microarray analysis, the brains of male pups obtained at PND 20 were fixed in Bouin's solution at room temperature overnight. Ten animals for each group were used except for the untreated control group with six animals.

Antibodies against vimentin (mouse monoclonal antibody, 1:200; Millipore Corporation, Billerica, MA), glial fibrillary acidic protein (GFAP, rabbit polyclonal antibody, 1:500; Dako, Glostrup, Denmark), Ret (rabbit polyclonal antibody, 1:50; Santa Cruz Biotechnology, Inc., Santa Cruz, CA), DCC (mouse monoclonal antibody, 1:40; Leica Microsystems GmbH), and oligodendrocyte specific protein (OSP, same as Cld11, rabbit polyclonal antibody, 1:200; Novus Biologicals, Inc., Co., Littleton, CO) were used for immunohistochemistry. For antigen retrieval, sections were heated in 10 mM citrate buffer in a microwave for 10 min before incubation with anti-vimentin and -DCC antibodies. Immunodetection was carried out using a VECTASTAIN® Elite ABC kit (Vector Laboratories Inc., Burlingame, CA) with 3,3′-diaminobenzidine/$H_2O_2$ for the chromogen as described elsewhere [13,14]. Sections were then counterstained with hematoxylin and coverslipped for microscopic examination.

Please cite this article in press as: Fujimoto H, et al. Increased cellular distribution of vimentin and Ret in the cingulum induced by developmental hypothyroidism in rat offspring maternally exposed to anti-thyroid agents. Reprod Toxicol (2012), http://dx.doi.org/10.1016/j.reprotox.2012.03.005

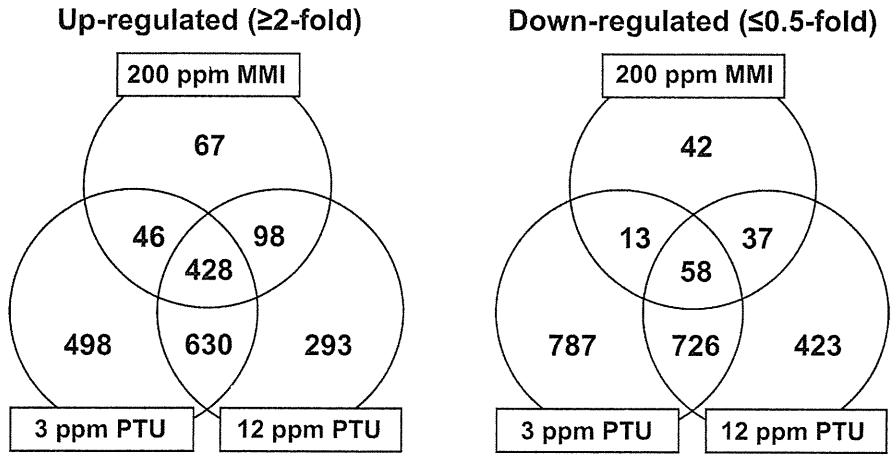


**Fig. 2.** Venn diagram of genes with altered expression in microarray analysis in response to maternal exposure to anti-thyroid agents. (Left) Up-regulated genes (≥2-fold). (Right) Down-regulated genes (≤0.5-fold).

### 2.7. Morphometry of immunolocalized cells

The number of immunoreactive cells was quantitatively measured by vimentin and Ret expression in white matter at the cingulum of the bilateral sides using two sections with an approximately 100 μm interval (i.e. four images per animal; Fig. 1), and values were normalized and expressed as those in the unit area ($cm^2$). GFAP-immunoreactive cells were similarly measured. For quantitative measurement of each immunoreactive cellular component containing vimentin, Ret and GFAP, digital photomicrographs at 100-fold magnification were taken using a BX51 microscope (Olympus Optical Co., Ltd., Tokyo, Japan) attached to a DP70 Digital Camera System (Olympus Optical Co.), and quantitative measurements were performed using WinROOF image analysis software 5.7 (Mitani Corp., Fukui, Japan). To evaluate immunoreactivity of DCC and Cld11 in white matter, staining intensity was scored as 0 (none), 1 (minimal), 2 (slight), 3 (moderate) and 4 (strong) by observation at 40-fold magnification.

### 2.8. Statistical analysis

Numerical data were assessed by one-way analysis of variance or the Kruskal–Wallis test following Bartlett's test. Statistically significant differences were analyzed by Dunnett's multiple test for comparison with that of the untreated control group. For grading immunohistochemical findings, scores of DCC and Cld11 expression were analyzed with the Mann-Whitney's *U*-test between the untreated control group and each anti-thyroid agent treated group.

## 3. Results

### 3.1. Global gene expression analysis

Fig. 2 shows the Venn diagram of genes with altered expression in microdissected cerebral white matter in treated groups in combination or individually in each treated group. Numerous common genes were found to be up- or down-regulated in two of the three treatment groups. The number of genes with up- or down-regulation in response to 3 ppm PTU was higher compared with that of 12 ppm PTU. The number of genes with

**Table 1**
List of representative genes associated with brain development showing up- or down-regulation common to treatments with MMI and PTU at both 3 and 12 ppm (≥2-fold, ≤0.5-fold).

| Accession no. | Gene title | Symbol | MMI | PTU, 3 ppm | PTU, 12 ppm |
|---|---|---|---|---|---|
| Up-regulated (20 genes) | | | | | |
| NM_052803 | ATPase, Cu++ transporting, alpha polypeptide | *Atp7a* | 5.02 | 11.39 | 11.09 |
| NM_001108322 | T-box 1 | *Tbx1* | 4.20 | 4.34 | 2.31 |
| NM_001191609 | Laminin, alpha 5 | *Lama5* | 4.11 | 11.57 | 9.35 |
| NM_031550 | Cyclin-dependent kinase inhibitor 2A | *Cdkn2a* | 3.59 | 2.70 | 3.37 |
| NM_001114330 | Glutamate receptor, metabotropic 1 | *Grm1* | 3.45 | 2.92 | 5.89 |
| (NM_001114330) | | | (3.01) | (2.85) | (2.88) |
| NM_023091 | gamma-Aminobutyric acid A receptor, epsilon | *Gabre* | 3.20 | 3.91 | 7.46 |
| NM_001107692 | Ephrin A4 | *Efna4* | 3.13 | 5.07 | 6.72 |
| NM_001002805 | Complement component 4a | *C4a* | 3.04 | 7.15 | 6.43 |
| NM_019328 | Nuclear receptor subfamily 4, group A, member 2 | *Nr4a2* | 2.97 | 2.87 | 4.92 |
| NM_001110099 | Ret proto-oncogene | *Ret* | 2.89 | 5.01 | 4.39 |
| NM_053629 | Follistatin-like 3 | *Fstl3* | 2.85 | 4.28 | 6.08 |
| NM_053708 | Gastrulation brain homeobox 2 | *Gbx2* | 2.82 | 4.73 | 4.09 |
| NM_019236 | Hairy and enhancer of split 2 | *Hes2* | 2.76 | 2.93 | 3.11 |
| NM_001109223 | Wingless-related MMTV integration site 16 | *Wnt16* | 2.71 | 2.42 | 3.82 |
| XM_001077495 | Nuclear receptor co-repressor 1 | *Ncor1* | 2.67 | 2.01 | 2.97 |
| NM_001012220 | Cation channel, sperm associated 2 | *Catsper2* | 2.54 | 6.69 | 4.56 |
| NM_001024275 | Ras association (RalGDS/AF-6) domain family 4 | *Rassf4* | 2.31 | 4.67 | 5.43 |
| NM_138900 | Complement component 1, s subcomponent | *C1s* | 2.12 | 3.31 | 3.88 |
| NM_031140 | Vimentin | *Vim* | 2.11 | 6.01 | 4.27 |
| NM_053555 | Vesicle-associated membrane protein 5 | *Vamp5* | 2.04 | 2.62 | 3.41 |
| Down-regulated (4 genes) | | | | | |
| NM_013107 | Bone morphogenetic protein 6 | *Bmp6* | 0.23 | 0.38 | 0.25 |
| NM_053759 | Sine oculis homeobox homolog 1 | *Six1* | 0.45 | 0.35 | 0.46 |
| NM_019280 | Gap junction membrane channel protein alpha 5 | *Gja5* | 0.46 | 0.16 | 0.28 |
| NM_133293 | GATA binding protein 3 | *Gata3* | 0.47 | 0.47 | 0.24 |

*Abbreviations:* MMI, 2-mercapto-1-methylimidazole; PTU, 6-propyl-2-thiouracil.

Please cite this article in press as: Fujimoto H, et al. Increased cellular distribution of vimentin and Ret in the cingulum induced by developmental hypothyroidism in rat offspring maternally exposed to anti-thyroid agents. Reprod Toxicol (2012), http://dx.doi.org/10.1016/j.reprotox.2012.03.005

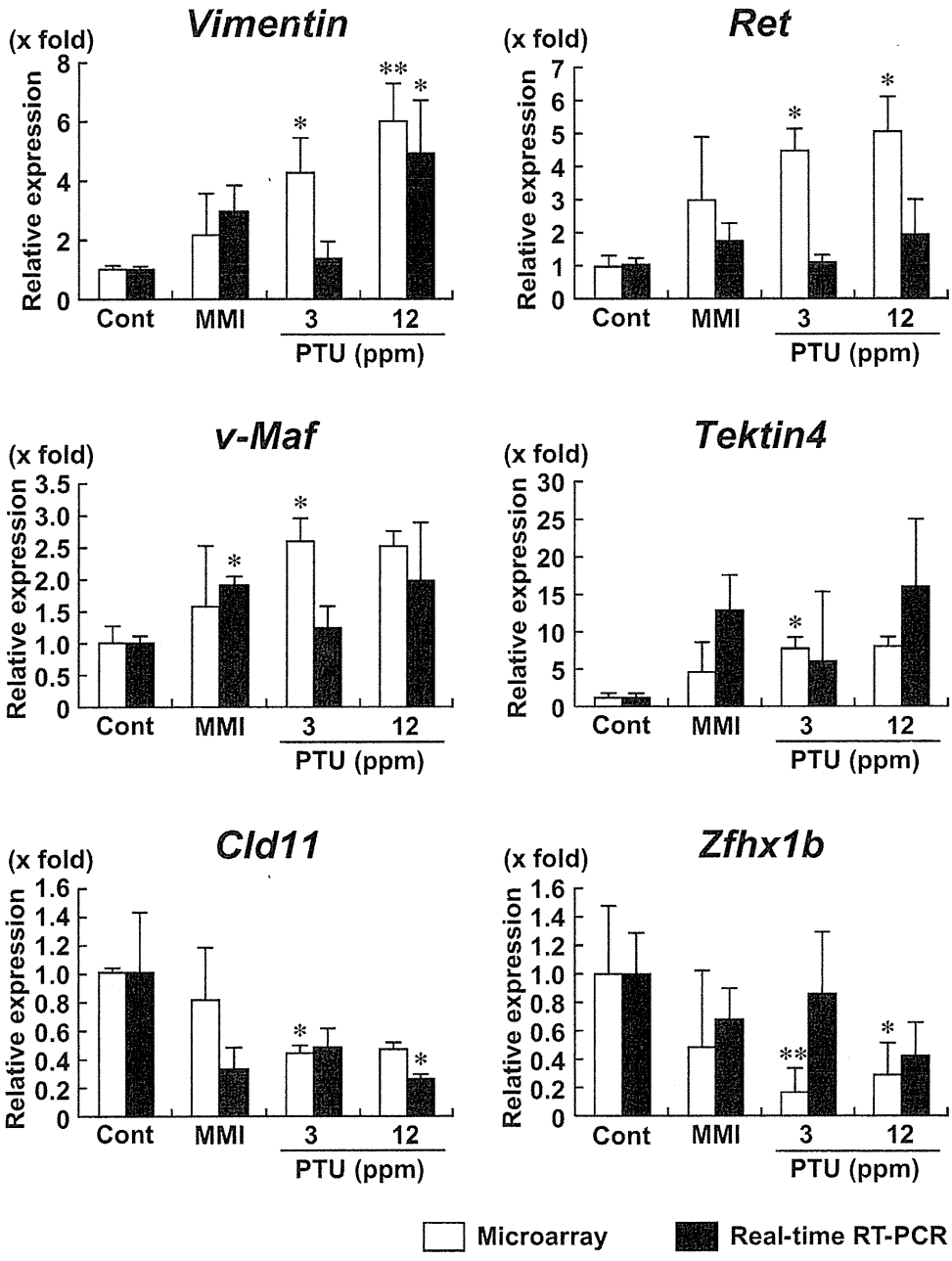


**Fig. 3.** Validation of mRNA expression of genes selected from microarray data ($n = 4$ in each group). *$P < 0.05$, **$P < 0.01$ vs. untreated controls.

up- or down-regulation in response to 200 ppm MMI was much lower compared with those of both PTU groups. Four hundred and eighty six common genes (428 up-regulated; 58 down-regulated) were identified with altered expression between MMI and both PTU groups (Fig. 2 and Supplementary data: Tables 1 and 2). Among these genes, the genes associated with central nervous system (CNS) development, cell differentiation and cell adhesion were commonly up- or down-regulated in response to anti-thyroid agents (Supplementary data: Tables 1 and 2). Twenty-four genes (20 up-regulated; 4 down-regulated) were related to CNS development involving glial cell differentiation, axon guidance, myelination, and cellular migration (Table 1). Among them, 12 up-regulated genes and two down-regulated genes showed PTU dose-dependent expression changes. For confirmation of microarray data, four genes that were up-regulated and two genes that were down-regulated in response to anti-thyroid agents were selected for mRNA expression analysis by real-time RT-PCR. Results are summarized in Fig. 3. All genes examined showed fluctuations in transcript levels in any of anti-thyroid agent treatment groups, which was similar to that of microarray data.

### 3.2. Immunolocalization of selected molecules in cerebral white matter

Immunohistochemical localization of vimentin, Ret, DCC and Cld11 was examined in the cerebral white matter. Within white

Please cite this article in press as: Fujimoto H, et al. Increased cellular distribution of vimentin and Ret in the cingulum induced by developmental hypothyroidism in rat offspring maternally exposed to anti-thyroid agents. Reprod Toxicol (2012), http://dx.doi.org/10.1016/j.reprotox.2012.03.005

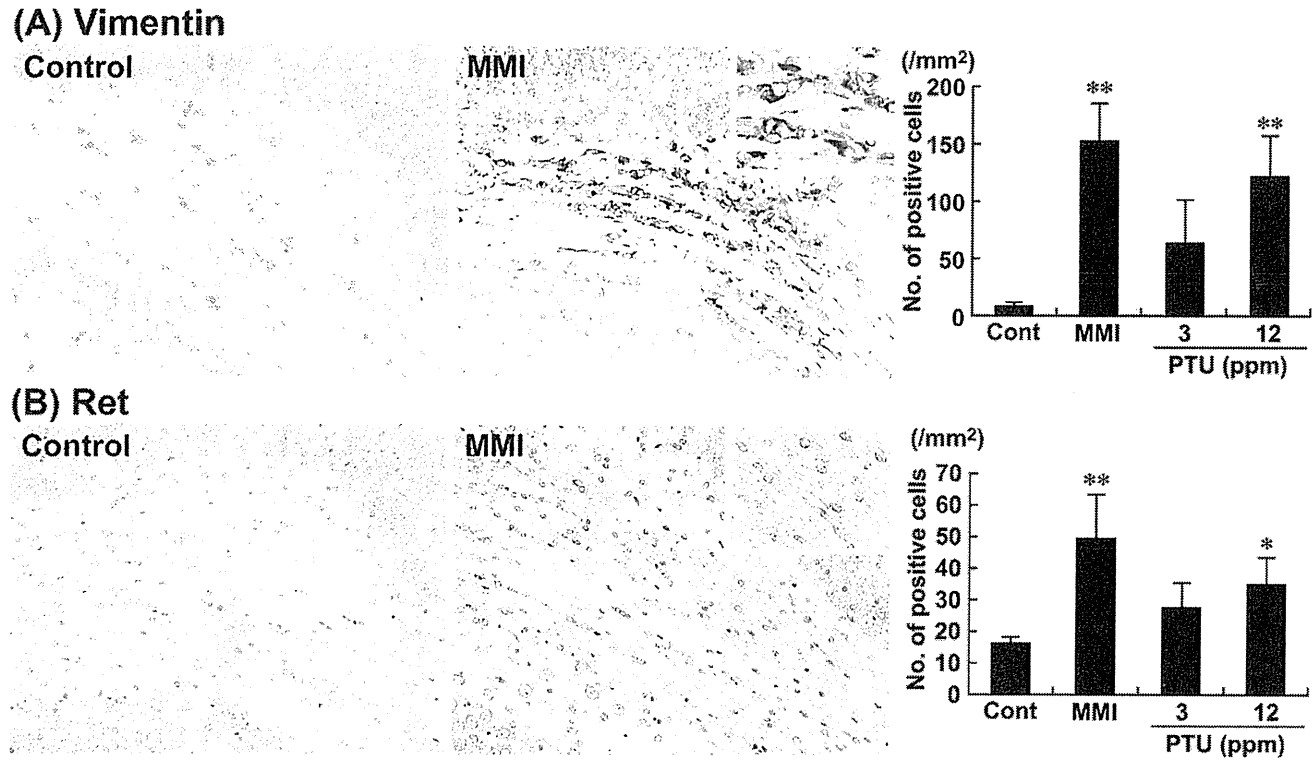


**Fig. 4.** Immunohistochemical distributions of vimentin- and Ret-positive cells in the while matter tissue. (A) Vimentin-immunoreactive cells in the cingulum. Untreated control animal (left) and MMI-treated animal (right). 200× magnification (inset: 400× magnification). Graph shows the mean number of positive cells within the cingulum at 200× magnification (untreated controls: $n = 6$; MMI and PTU groups: $n = 10$). $^{**}P < 0.01$ vs. untreated controls. (B) Ret-immunoreactive cells in the cingulum. Untreated control animal (left), MMI-treated animal (right). 200× magnification (inset: 400× magnification). Graph shows the mean number of positive cells within the cingulum at 100× magnification (untreated controls: $n = 6$; MMI and PTU groups: $n = 10$). $^{*}P < 0.05$, $^{**}P < 0.01$ vs. untreated controls.

matter tissues, vimentin-immunoreactive cells were scarcely distributed in untreated control animals (Fig. 4A). After treatment with anti-thyroid agents, the distribution of vimentin-positive cells were mainly observed in the cingulum with a statistically significant increase in number with MMI and 12 ppm PTU treatments (Fig. 4A).

Ret-immunoreactive cells were mainly observed in white matter tissues of untreated control animals (Fig. 4B). After treatment with anti-thyroid agents, Ret-positive cells were mainly observed in the cingulum with a statistically significant increase in number with MMI and 12 ppm PTU treatments (Fig. 4B).

DCC showed diffuse immunoreactivity in white matter, indicating myelin sheaths with a statistically significant increase in the intensity scores of animals treated with MMI and 12 ppm PTU as compared with those of the untreated control (Fig. 5A).

Diffuse Cld11-immunoreactivity was observed in white matter, indicating myelin sheaths (Fig. 5B). The immunoreactivity showed a statistically significant increase in the intensity score of animals treated with MMI as compared with that of the untreated control (Fig. 5B).

### 3.3. Immunolocalization of GFAP

To investigate the cell type of vimentin-positive cells, cellular distribution of GFAP immunoreactivity was analyzed as a marker of astrocytes. Untreated control animals showed scattered distribution of GFAP-immunoreactive cells in cerebral white matter, and the number of GFAP-immunoreactive cells was higher compared with that of vimentin-positive cells. GFAP-immunoreactive cells showed a similar distribution to that of vimentin-immunoreactive cells, with accumulated distribution in the cingulum (Fig. 6). After treatment with anti-thyroid agents, the number of GFAP-positive cells was significantly increased in animals treated with MMI and 12 ppm PTU.

## 4. Discussion

In our previous study [16], maternal exposure to MMI and PTU induced typical hypothyroidism-related changes in the concentration of thyroid-related hormones, and variability in the distribution of hippocampal CA1 pyramidal neurons due to neuronal mismigration [16]. With regard to thyroid hormone-related changes in functions or structures in glial cell populations, gene expression alternations have been reported in myelin-related protein genes related to oligodendrocytes [20,21], as well as in enzymes or cytoskeletal components related to astrocytes [22–24]. Therefore, both oligodendrocytes and astrocytes could also be the target of developmental hypothyroidism. We, in the above-mentioned study [16], also observed changes in white matter structures with hypoplasia due to impaired oligodendroglial development as previously reported [2,9]. Using the same study samples, we, in the present study, analyzed immunohistochemical distribution of molecules that showed fluctuations in gene expression from microarray analysis of cerebral white matter tissue collected using microdissection targeting oligodendrocytes and astrocytes. This is the first report to use microarray analysis of gene expression changes induced by developmental hypothyroidism in white matter, whereas there have been such approaches for the study of cerebral cortex and hippocampal substructures [15,25,26]. We found that anti-thyroid agents caused fluctuations in a number of genes associated with CNS development involving glial cell differentiation, axon guidance, myelination, and cellular migration as listed in Table 1. Among them, vimentin, Ret, DCC and Cld11

Please cite this article in press as: Fujimoto H, et al. Increased cellular distribution of vimentin and Ret in the cingulum induced by developmental hypothyroidism in rat offspring maternally exposed to anti-thyroid agents. Reprod Toxicol (2012), http://dx.doi.org/10.1016/j.reprotox.2012.03.005

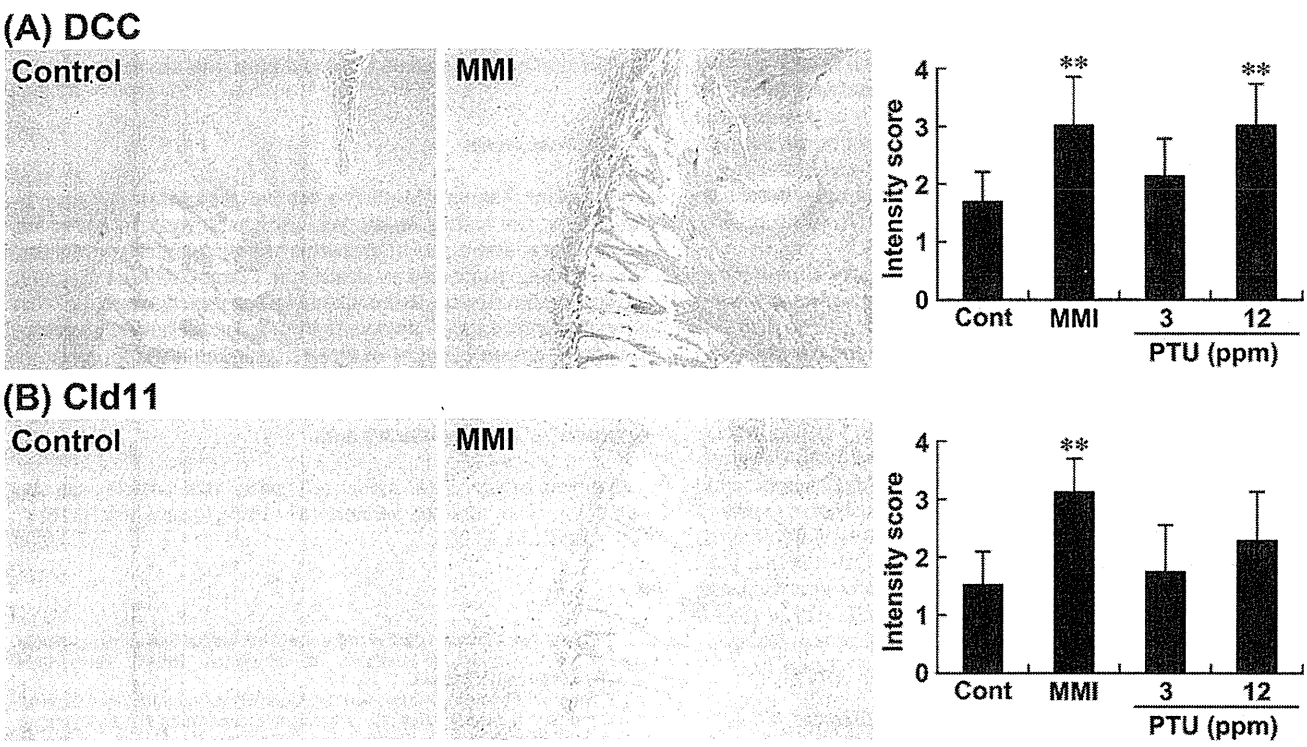


**Fig. 5.** Immunohistochemical distributions of DCC- and Cld11 in the while matter tissue. (A) DCC-immunoreactivity in the myelin sheath of the external capsule, internal capsule, and fimbria of the hippocampus. Untreated control animal (left), MMI-treated animal (right). 40× magnification. Graph shows the mean intensity score of immunoreactivity at 40× magnification (untreated controls: $n = 6$; MMI and PTU groups: $n = 10$). $^{**}P < 0.01$ vs. untreated controls. (B) Cld11-immunoreactivity in the myelin sheath of the external capsule, internal capsule, and fimbria of the hippocampus. Untreated control animal (left), MMI-treated animal (right). 40× magnification. Graph shows the mean intensity score of immunoreactivity at 40× magnification (untreated controls: $n = 6$; MMI and PTU groups: $n = 10$). $^{**}P < 0.01$ vs. untreated controls.

showed immunohistochemical distribution changes in the cerebral white matter of offspring after maternal exposure to PTU and MMI.

Cld11 is a four-transmembrane protein, which is primarily expressed in oligodendrocytes of the CNS and is the third most abundant CNS myelin protein [27–29]. Cld11 is involved in the formation of intramembranous tight junctions within the myelin sheath [30]. It is known that developmental hypothyroidism results in continued reduction of oligodendrocytes in the CC region from PND 10 [2]. In vitro study has shown that Cld11-overexpression results in induction of oligodendrocyte proliferation [31]. This result indicates that the overexpression of Cld11 at PND 20 is a compensatory response to decrease numbers of oligodendrocytes. However, mRNA levels were inconsistently decreased, suggesting involvement of post-transcriptional events such as those regulating mRNA stability and protein turnover.

DCC is a transmembrane receptor for netrin-1 via the fourth fibronectin type III domain [32]. Netrin-1 is a secreted protein, which elicits both attractive and repulsive responses in axonal guidance, neuronal migration and oligodendroglial migration depending on the homomeric or heteromeric combination of receptor dimers including DCC and Unc5 [33–35]. Netrin-1 signaling via DCC mediates growth cone extension and myelin sheath formation [36,37]. Therefore, increased expression of DCC in the myelin sheath at PND 20 induced by developmental hypothyroidism in the present study suggests a compensatory increase in response to suppression of myelin sheath formation [2]. However,


**Fig. 6.** Immunohistochemical distributions of GFAP-positive cells in the cingulum. Untreated control animal (left), MMI-treated animal (right). 200× magnification. Graph shows the mean number of positive cells within the cingulum at 200× magnification (untreated controls: $n = 6$; MMI and PTU groups: $n = 10$). $^{*}P < 0.05$, $^{**}P < 0.01$ vs. untreated controls.

Please cite this article in press as: Fujimoto H, et al. Increased cellular distribution of vimentin and Ret in the cingulum induced by developmental hypothyroidism in rat offspring maternally exposed to anti-thyroid agents. Reprod Toxicol (2012), http://dx.doi.org/10.1016/j.reprotox.2012.03.005

DCC has an alternative function to drive cell death independent of both mitochondria-dependent and death receptor/caspase-8 pathways [38,39]. Moreover, DCC induces cell death in the absence of netrin-1 [40]. Because we did not find an increase in netrin-1 transcript levels using microarray analysis, it is possible that increased ligand-free DCC may lead to glial cell apoptosis. Progressive decrease in the CC area and the number of oligodendrocytes in this area during maturation after developmental hypothyroidism suggests the involvement of apoptosis due to increased ligand-free DCC [2,16].

Ret is a receptor protein–tyrosine kinase of glial cell line-derived neurotrophic factor (GDNF), a member of the transforming growth factor-β family [41]. GDNF signals play a critical role in development of the entire nervous system, kidney morphogenesis and spermatogenesis. While the functional relevance of Ret in oligodendrocytes has not been reported, this molecule is expressed in progenitor and immature oligodendrocytes in vitro and mediates cell proliferation induced by GDNF treatment [42]. Therefore, increased expression of Ret on PND 20 proceeding developmental hypothyroidism suggests a compensatory increase in response to decreased numbers of oligodendrocytes [2]. However, Ret induces cell death in the absence of its ligand similar to that of DCC [43]. Because we did not find an increase in GDNF transcript levels using microarray analysis, a progressive decrease in the size of the CC area and its oligodendrocyte density during maturation suggests involvement of apoptosis due to the increase of ligand-free Ret [2,16].

Vimentin is a member of the intermediate filament family of proteins. In the brain, this molecule is expressed in immature astrocytes during development [44–46]. Reactive astrocytes that are activated immature astrocytes during gliosis processes in response to injuries of CNS tissue also express vimentin [47,48]. Reactive astrocytes also express GFAP similar to that of mature astrocytes [47,48], suggesting that immature astrocytes can express both of vimentin and GFAP. On the other hand, developmental hypothyroidism leads to increase in vimentin expression in fetal rat brains [23]. Increase of GFAP-expression was also reported after developmental hypothyroidism in the CC region on PND 15 [49]. These results may suggest that developmental hypothyroidism increases the immature population of astrocytes. In the present study, vimentin-immunoreactive cells showed similar localization to those positive for GFAP. Therefore, a larger population of vimentin-positive cells in the cingulum induced by developmental hypothyroidism was considered to consist of immature astrocytes resembling reactive astrocytes. Interestingly, we previously reported frequent induction of subcortical band heterotopia in the CC, manifested by the appearance of aberrant cortical tissue in this anatomical area, in hypothyroid animals identical to the present study [16]. Anatomical location of this heterotopic tissue was close to the cingulum accumulating immature astrocytes, suggesting an etiological relation between the two. Alternatively, the increased immature astrocytes may simply be the reactive change in response to reduced oligodendrocytes due to developmental hypothyroidism [2,16,49]. However, developmental hypothyroidism may affect differentiation of neuronal progenitor cells, thereby inhibiting differentiation into oligodendrocytes, and instead, facilitating astrocytic differentiation during gliogenesis.

In conclusion, focusing on white matter development, we found aberrant expression of molecules associated with brain development after maternal exposure to anti-thyroid agents. Immunohistochemically, we found increased expression of Cld11, DCC, Ret and vimentin in white matter. Among them, vimentin and Ret were expressed in immature astrocytes and oligodendrocytes, respectively. Both positive cell populations were mainly distributed in the cingulum with the largest area of white matter. Because vimentin- and Ret-positive cells can be quantitatively evaluated, these molecules may be useful markers of glial cells, which respond to developmental exposure to thyroid hormone-disrupting chemicals.

## Acknowledgments

We thank Tomomi Morikawa for her technical assistance in conducting the animal study. We also thank Ayako Kaneko for her technical assistance in preparing the histological specimens. This work was supported by Health and Labour Sciences Research Grants (Research on the Risk of Chemical Substances) from the Ministry of Health, Labour and Welfare of Japan. All authors disclose that there are no conflicts of interest that could inappropriately influence the outcome of the present study.

## Appendix A. Supplementary data

Supplementary data associated with this article can be found, in the online version, at http://dx.doi.org/10.1016/j.reprotox.2012.03.005.

## References

[1] Porterfield SP. Thyroidal dysfunction and environmental chemicals—potential impact on brain development. Environmental Health Perspectives 2000;108(Suppl. 3):433–8.
[2] Schoonover CM, Seibel MM, Jolson DM, Stack MJ, Rahman RJ, Jones SA, et al. Thyroid hormone regulates oligodendrocyte accumulation in developing rat brain white matter tracts. Endocrinology 2004;145:5013–20.
[3] Montero-Pedrazuela A, Venero C, Lavado-Autric R, Fernández-Lamo I, García-Verdugo JM, Bernal J, et al. Modulation of adult hippocampal neurogenesis by thyroid hormones: implications in depressive-like behavior. Molecular Psychiatry 2006;11:361–71.
[4] de Escobar GM, Obregón MJ, del Rey FE. Iodine deficiency and brain development in the first half of pregnancy. Public Health Nutrition 2007;10:1554–70.
[5] Comer CP, Norton S. Effects of perinatal methimazole exposure on a developmental test battery for neurobehavioral toxicity in rats. Toxicology and Applied Pharmacology 1982;63:133–41.
[6] Akaike M, Kato N, Ohno H, Kobayashi T. Hyperactivity and spatial maze learning impairment of adult rats with temporary neonatal hypothyroidism. Neurotoxicology and Teratology 1991;13:317–22.
[7] Guadaño Ferraz A, Escobar del Rey F, Morreale de Escobar G, Innocenti GM, Berbel P. The development of the anterior commissure in normal and hypothyroid rats. Brain Research Developmental Brain Research 1994;81:293–308.
[8] Lavado-Autric R, Ausó E, García-Velasco JV, Arufe Mdel C, Escobar del Rey F, Berbel P, et al. Early maternal hypothyroxinemia alters histogenesis and cerebral cortex cytoarchitecture of the progeny. Journal of Clinical Investigation 2003;111:954–7.
[9] Goodman JH, Gilbert ME. Modest thyroid hormone insufficiency during development induces a cellular malformation in the corpus callosum: a model of cortical dysplasia. Endocrinology 2007;148:2593–7.
[10] Shibutani M, Uneyama C, Miyazaki K, Toyoda K, Hirose M. Methacarn fixation: a novel tool for analysis of gene expressions in paraffin-embedded tissue specimens. Laboratory Investigation 2000;80:199–208.
[11] Uneyama C, Shibutani M, Masutomi N, Takagi H, Hirose M. Methacarn fixation for genomic DNA analysis in microdissected, paraffin-embedded tissue specimens. Journal of Histochemistry and Cytochemistry 2002;50:1237–45.
[12] Takagi H, Shibutani M, Kato N, Fujita H, Lee KY, Takigami S, et al. Microdissected region-specific gene expression analysis with methacarn-fixed, paraffin-embedded tissues by real-time RT-PCR. Journal of Histochemistry and Cytochemistry 2004;52:903–13.
[13] Shibutani M, Lee KY, Igarashi K, Woo GH, Inoue K, Nishimura T, et al. Hypothalamus region-specific global gene expression profiling in early stages of central endocrine disruption in rat neonates injected with estradiol benzoate or flutamide. Developmental Neurobiology 2007;67:253–69.
[14] Woo GH, Takahashi M, Inoue K, Fujimoto H, Igarashi K, Kanno J, et al. Cellular distributions of molecules with altered expression specific to thyroid proliferative lesions developing in a rat thyroid carcinogenesis model. Cancer Science 2009;100:617–25.
[15] Saegusa Y, Woo GH, Fujimoto H, Inoue K, Takahashi M, Hirose M, et al. Gene expression profiling and cellular distribution of molecules with altered expression in the hippocampal CA1 region after developmental exposure to anti-thyroid agents in rats. Journal of Veterinary Medical Science 2010;72:187–95.
[16] Shibutani M, Woo GH, Fujimoto H, Saegusa Y, Takahashi M, Inoue K, et al. Assessment of developmental effects of hypothyroidism in rats from in utero and lactation exposure to anti-thyroid agents. Reproductive Toxicology 2009;28:297–307.

Please cite this article in press as: Fujimoto H, et al. Increased cellular distribution of vimentin and Ret in the cingulum induced by developmental hypothyroidism in rat offspring maternally exposed to anti-thyroid agents. Reprod Toxicol (2012), http://dx.doi.org/10.1016/j.reprotox.2012.03.005

[17] Masutomi N, Shibutani M, Takagi H, Uneyama C, Takahashi N, Hirose M. Impact of dietary exposure to methoxychlor, genistein, or diisononyl phthalate during the perinatal period on the development of the rat endocrine/reproductive systems in later life. Toxicology 2003;192:149–70.
[18] Nakamura R, Teshima R, Hachisuka A, Sato Y, Takagi K, Nakamura R, et al. Effects of developmental hypothyroidism induced by maternal administration of methimazole or propylthiouracil on the immune system of rats. International Immunopharmacology 2007;7:1630–8.
[19] Lee KY, Shibutani M, Inoue K, Kuroiwa K, U M, Woo GH, et al. Methacarn fixation—effects of tissue processing and storage conditions on detection of mRNAs and proteins in paraffin-embedded tissues. Analytical Biochemistry 2006;351:36–43.
[20] Ibarrola N, Rodríguez-Peña A. Hypothyroidism coordinately and transiently affects myelin protein gene expression in most rat brain regions during postnatal development. Brain Research 1997;752:285–93.
[21] Barradas PC, Vieira RS, De Freitas MS. Selective effect of hypothyroidism on expression of myelin markers during development. Journal of Neuroscience Research 2001;66:254–61.
[22] Farwell AP, Dubord-Tomasetti SA. Thyroid hormone regulates the expression of laminin in the developing rat cerebellum. Endocrinology 1999;140:4221–7.
[23] Evans IM, Pickard MR, Sinha AK, Leonard AJ, Sampson DC, Ekins RP. Influence of maternal hyperthyroidism in the rat on the expression of neuronal and astrocytic cytoskeletal proteins in fetal brain. Journal of Endocrinology 2002;175:597–604.
[24] Dasgupta A, Das S, Sarkar PK. Thyroid hormone promotes glutathione synthesis in astrocytes by up regulation of glutamate cysteine ligase through differential stimulation of its catalytic and modulator subunit mRNAs. Free Radical Biology and Medicine 2007;42:617–26.
[25] Royland JE, Parker JS, Gilbert ME. A genomic analysis of subclinical hypothyroidism in hippocampus and neocortex of the developing rat brain. Journal of Neuroendocrinology 2008;20:1319–38.
[26] Kobayashi K, Akune H, Sumida K, Saito K, Yoshioka T, Tsuji R. Perinatal exposure to PTU decreases expression of Arc, Homer 1, Egr 1 and Kcna 1 in the rat cerebral cortex and hippocampus. Brain Research 2009;1264:24–32.
[27] Bronstein JM, Popper P, Micevych PE, Farber DB. Isolation and characterization of a novel oligodendrocyte-specific protein. Neurology 1996;47:772–8.
[28] Bronstein JM, Micevych PE, Chen K. Oligodendrocyte-specific protein (OSP) is a major component of CNS myelin. Journal of Neuroscience Research 1997;50:713–20.
[29] Morita K, Sasaki H, Fujimoto K, Furuse M, Tsukita S. Claudin-11/OSP-based tight junctions of myelin sheaths in brain and Sertoli cells in testis. Journal of Cell Biology 1999;145:579–88.
[30] Gow A, Southwood CM, Li JS, Pariali M, Riordan GP, Brodie SE, et al. CNS myelin and sertoli cell tight junction strands are absent in Osp/claudin-11 null mice. Cell 1999;99:649–59.
[31] Tiwari-Woodruff SK, Buznikov AG, Vu TQ, Micevych PE, Chen K, Kornblum HI, et al. OSP/claudin-11 forms a complex with a novel member of the tetraspanin super family and beta1 integrin and regulates proliferation and migration of oligodendrocytes. Journal of Cell Biology 2001;153:295–305.
[32] Kruger RP, Lee J, Li W, Guan KL. Mapping netrin receptor binding reveals domains of Unc5 regulating its tyrosine phosphorylation. Journal of Neuroscience 2004;24:10826–34.
[33] Serafini T, Colamarino SA, Leonardo ED, Wang H, Beddington R, Skarnes WC, et al. Netrin-1 is required for commissural axon guidance in the developing vertebrate nervous system. Cell 1996;87:1001–14.
[34] Alcántara S, Ruiz M, De Castro F, Soriano E, Sotelo C. Netrin 1 acts as an attractive or as a repulsive cue for distinct migrating neurons during the development of the cerebellar system. Development 2000;127:1359–72.
[35] Spassky N, de Castro F, Le Bras B, Heydon K, Quéraud-LeSaux F, Bloch-Gallego E, et al. Directional guidance of oligodendroglial migration by class 3 semaphorins and netrin-1. Journal of Neuroscience 2002;22:5992–6004.
[36] Fazeli A, Dickinson SL, Hermiston ML, Tighe RV, Steen RG, Small CG, et al. Phenotype of mice lacking functional Deleted in colorectal cancer (Dcc) gene. Nature 1997;386:796–804.
[37] Rajasekharan S, Baker KA, Horn KE, Jarjour AA, Antel JP, Kennedy TE. Netrin 1 and Dcc regulate oligodendrocyte process branching and membrane extension via Fyn and RhoA. Development 2009;136:415–26.
[38] Forcet C, Ye X, Granger L, Corset V, Shin H, Bredesen DE, et al. The dependence receptor DCC (deleted in colorectal cancer) defines an alternative mechanism for caspase activation. Proceedings of the National Academy of Sciences of the United States of America 2001;98:3416–21.
[39] Furne C, Corset V, Hérincs Z, Cahuzac N, Hueber AO, Mehlen P. The dependence receptor DCC requires lipid raft localization for cell death signaling. Proceedings of the National Academy of Sciences of the United States of America 2006;103:4128–33.
[40] Mehlen P, Rabizadeh S, Snipas SJ, Assa-Munt N, Salvesen GS, Bredesen DE. The DCC gene product induces apoptosis by a mechanism requiring receptor proteolysis. Nature 1998;395:801–4.
[41] Sariola H, Saarma M. Novel functions and signalling pathways for GDNF. Journal of Cell Science 2003;116:3855–62.
[42] Strelau J, Unsicker K. GDNF family members and their receptors: expression and functions in two oligodendroglial cell lines representing distinct stages of oligodendroglial development. Glia 1999;26:291–301.
[43] Bordeaux MC, Forcet C, Granger L, Corset V, Bidaud C, Billaud M, et al. The RET proto-oncogene induces apoptosis: a novel mechanism for Hirschsprung disease. EMBO Journal 2000;19:4056–63.
[44] Pixley SK, de Vellis J. Transition between immature radial glia and mature astrocytes studied with a monoclonal antibody to vimentin. Brain Research 1984;317:201–9.
[45] Ciesielski-Treska J, Goetschy JF, Ulrich G, Aunis D. Acquisition of vimentin in astrocytes cultured from postnatal rat brain. Journal of Neurocytology 1988;17:79–86.
[46] Alonso G. Proliferation of progenitor cells in the adult rat brain correlates with the presence of vimentin-expressing astrocytes. Glia 2001;34:253–66.
[47] Pekny M, Wilhelmsson U, Bogestål YR, Pekna M. The role of astrocytes and complement system in neural plasticity. International Review of Neurobiology 2007;82:95–111.
[48] Eddleston M, Mucke L. Molecular profile of reactive astrocytes—implications for their role in neurologic disease. Neuroscience 1993;54:15–36.
[49] Sharlin DS, Bansal R, Zoeller RT. Polychlorinated biphenyls exert selective effects on cellular composition of white matter in a manner inconsistent with thyroid hormone insufficiency. Endocrinology 2006;147:846–58.

Please cite this article in press as: Fujimoto H, et al. Increased cellular distribution of vimentin and Ret in the cingulum induced by developmental hypothyroidism in rat offspring maternally exposed to anti-thyroid agents. Reprod Toxicol (2012), http://dx.doi.org/10.1016/j.reprotox.2012.03.005

GModel
RTX66861–12
ARTICLE IN PRESS

Reproductive Toxicology xxx (2012) xxx–xxx

Contents lists available at SciVerse ScienceDirect

Reproductive Toxicology

journal homepage: www.elsevier.com/locate/reprotox

# Reversible aberration of neurogenesis affecting late-stage differentiation in the hippocampal dentate gyrus of rat offspring after maternal exposure to manganese chloride

Takumi Ohishi[a,b], Liyun Wang[a], Hirotoshi Akane[a], Ayako Shiraki[a], Ken Goto[b], Yoshiaki Ikarashi[c], Kazuhiko Suzuki[a], Kunitoshi Mitsumori[a], Makoto Shibutani[a,*]

[a] Laboratory of Veterinary Pathology, Tokyo University of Agriculture and Technology, 3-5-8 Saiwai-cho, Fuchu-shi, Tokyo 183-8509, Japan
[b] Gotemba Laboratory, Bozo Research Center Inc., 1284 Kamado, Gotemba-shi, Shizuoka 412-0039, Japan
[c] Division of Environmental Chemistry, National Institute of Health Sciences, 1-18-1 Kamiyoga, Setagaya-ku, Tokyo 158-8501, Japan

ARTICLE INFO

*Article history:*
Received 13 November 2011
Received in revised form 15 March 2012
Accepted 25 April 2012
Available online xxx

*Keywords:*
Manganese
Developmental neurotoxicity
Hippocampal dentate gyrus
Thyroid hormone

ABSTRACT

To examine the effects of developmental manganese (Mn)-exposure on hippocampal neurogenesis, pregnant rats were treated with $MnCl_2 \cdot 4H_2O$ in the diet at 32, 160 or 800 ppm from gestation day 10 to day 21 after delivery. Serum concentrations of thyroid-related hormones were examined in offspring exposed to $MnCl_2 \cdot 4H_2O$ at 800 or 1600 ppm. Immunohistochemical analysis revealed increased doublecortin-positive cells in the subgranular zone of the dentate gyrus on postnatal day (PND) 21 following exposure to $MnCl_2 \cdot 4H_2O$ at 800 ppm, indicating an increase of type-3 progenitor or immature granule cells. Reelin-positive cells, suggestive of γ-aminobutyric acid-ergic interneurons in the dentate hilus, also increased at 800 ppm on PND 21. Brain Mn concentrations increased in offspring on PND 21 at 160 and 800 ppm, whereas brain concentrations in the dams were unchanged. Serum concentrations of triiodothyronine and thyroxine decreased at 800 and 1600 ppm, whereas thyroid-stimulating hormone increased only after exposure at 800 ppm. All changes disappeared on PND 77. Thus, maternal exposure to $MnCl_2 \cdot 4H_2O$ at 800 ppm mildly and reversibly affects neurogenesis targeting late-stage differentiation in the hippocampal dentate gyrus of rat offspring. Direct effects of accumulated Mn in the developing brain might be implicated in the mechanism of the development of aberrations in neurogenesis; however, indirect effects through thyroid hormone fluctuations might be rather minor.



## 1. Introduction

Manganese (Mn) is known as an essential trace metal and is needed for normal immune function, regulation of blood sugar and cellular energy, reproduction, digestion, bone growth, and aid in the defense mechanisms against free radicals [1]. Although natural Mn deficiency is rare, Mn-induced neurotoxicity by excess exposure known as manganism is similar to Parkinson's disease and has been well described [2,3].

Estimated safe and adequate daily dietary intake (ESADDI) of Mn has been estimated at approximately 0.6 mg/day for individuals 7–12 months of age, 1.2 mg/day for those 1–3 years of age, 1.5 mg/day for those 4–8 years of age and 2–5 mg/day for adults. On the other hand, the ESADDI for newborns has been estimated to be less than that for adults or children at 0.003 mg/day [1,3]. Several experimental studies have found that neonatal animals were more sensitive to Mn-induced neurotoxicity than adult animals in behavioral tests and on brain neurochemistry [4]. However, the risk of Mn-induced neurotoxicity during both pre- and postnatal periods has received relatively little attention and there are few studies using histopathological evaluation.

It has been suggested that Mn might also affect thyroid hormone homeostasis [5]. Thyroid hormones are critically involved in the growth, development and function of the central nervous system [6]. Using a rat model of developmental hypothyroidism, we have recently detected an increase of reelin-expressing γ-aminobutyric acid (GABA)ergic interneurons displaying an immature phenotype in the dentate hilus that was sustained through to the adult stage, as well as increased apoptosis and decreased cell proliferation

*Abbreviations:* DCX, doublecortin; ESADDI, estimated safe and adequate daily dietary intake; GABA, γ-aminobutyric acid; GAD67, glutamic acid decarboxylase 67; GD, gestation day; GFAP, glial fibrillary acidic protein; Mn, manganese; NeuN, neuron-specific nuclear protein; PCNA, proliferating cell nuclear antigen; PND, postnatal day; SGZ, subgranular zone; Tbr2, T box brain 2; TSH, thyroid-stimulating hormone; TUNEL, terminal deoxynucleotidyl transferase dUTP nick end labeling; $T_3$, triiodothyronine; $T_4$, thyroxine.

* Corresponding author. Tel.: +81 42 367 5874; fax: +81 42 367 5771.
*E-mail address:* mshibuta@cc.tuat.ac.jp (M. Shibutani).

0890-6238/$ – see front matter © 2012 Elsevier Inc. All rights reserved.
http://dx.doi.org/10.1016/j.reprotox.2012.04.009

Please cite this article in press as: Ohishi T, et al. Reversible aberration of neurogenesis affecting late-stage differentiation in the hippocampal dentate gyrus of rat offspring after maternal exposure to manganese chloride. Reprod Toxicol (2012), http://dx.doi.org/10.1016/j.reprotox.2012.04.009

**Table 1**
Culling and number of animals examined in Experiment 1.

| | Per litter | Per group (dams = 8) |
|---|---|---|
| PND 4 | | |
| Culling | Kept 4 males and 4 females | Kept 32 males and 32 females |
| PND 21 | | |
| Animals subjected to necropsy | 2 males and 2 females | 16 males and 16 females |
| Immunohistochemical analysis | 1 or 2 males | 10 males |
| Analyses of Mn concentrations and real-time RT-PCR | 1 male | 6 males |
| PND 77 | | |
| Animals subjected to necropsy | 2 males and 2 females | 16 males and 16 females |
| Immunohistochemical analysis | 1 or 2 males | 10 males |
| Analysis of Mn concentrations | 1 male | 6 males |

*Abbreviation*: PND, postnatal day.

suggestive of impaired neurogenesis in the neuroblast-producing subgranular zone (SGZ) [7]. Thus, the concern about effects on neurogenesis associated with changes in thyroid-related hormones arises in the case of developmental Mn-exposure.

Within the hippocampal formation, the dentate gyrus is a unique structure that can continue neurogenesis throughout the lifetime and that is a well-known target of developmental hypothyroidism [8]. The dentate gyrus is crucial for higher brain functions such as learning and memory, and malformation and malfunction of the dentate gyrus are associated with neurological and psychiatric disorders [9]. The dentate gyrus is known for its ongoing neurogenesis at the SGZ throughout postnatal life [10,11], and GABAergic interneurons in the hilus can control neurogenesis [7,12]. Reelin is a secreted extracellular matrix glycoprotein that plays a critical role in neuronal migration and positioning during brain development [13]. During the early postnatal life, reelin expression becomes established in a subpopulation of GABAergic interneurons in the dentate gyrus, with a high density in the hilus and along the base of the granule cell layer [14], where reelin is maintained throughout adult life [15,16]. In the interneurons, reelin modulates dentate granule cell progenitor migration to maintain normal dentate granule cell integration in the neonatal and adult mammalian dentate gyrus [17].

Reproduction studies and developmental neurotoxicity studies require large numbers of animals for detection of subtle dose–response changes. However, for screening purposes of many new chemicals, smaller scale studies, preferably with short-term experiments, need to be established. To establish a rapid screening system for developmental neurotoxicants, we focused on the neurogenesis and its regulatory system in the dentate gyrus using rodent models [7,18]. We hypothesize that monitoring of the dentate gyrus may provide a valuable tool for the detection of developmental neurotoxicants.

In the present study, to elucidate the effects of developmental exposure to Mn on neurogenesis, distribution of granule cell lineages as well as their proliferation and apoptosis in the SGZ and reelin-producing interneurons in the hilus of the hippocampal dentate gyrus were analyzed in the offspring of rats exposed to Mn during pregnancy and lactation periods in a small scale animal study. Furthermore, to clarify the relation of thyroid function to the Mn-induced brain effect, serum concentrations of thyroid-related hormones were also analyzed in Mn-exposed offspring.

## 2. Materials and methods

### 2.1. Chemicals and animals

Manganese chloride tetrahydrate ($MnCl_2{\cdot}4H_2O$; CAS No. 13446-34-9) was purchased from Sigma–Aldrich Japan K.K. (Tokyo, Japan). Pregnant Crl:CD®(SD) rats were purchased from Charles River Japan Inc. (Yokohama, Japan) at gestation day (GD) 1 (appearance of vaginal plugs was designated as GD 0). Pregnant rats were housed individually in mesh cages in an air-conditioned animal room (temperature: 23 ± 2 °C; relative humidity: 45 ± 10%) with a 12-h light/dark cycle and allowed *ad libitum* access to food and tap water. Pregnant rats were then housed individually in plastic cages with wood chip bedding from GD 17, and after delivery, dams with their litter were similarly housed to postnatal day (PND) 21 (where PND 0 is the day of delivery). Dams and pups were allowed *ad libitum* access to food and tap water. Pregnant rats were fed a CRF-1 basal diet (Oriental Yeast Co., Ltd.) from GD 1 to GD 10. All offspring consumed the CRF-1 basal diet and tap water *ad libitum* from PND 21 onwards. Mn concentration in the basal diet was 7.27 mg/100 g and that of the tap water was below the lower detection limit.

All procedures of this study were conducted in compliance with the *Guidelines for Proper Conduct of Animal Experiments* (Science Council of Japan, June 1, 2006) and according to the protocol approved by the Animal Care and Use Committee at BOZO Research Center Inc. All efforts were made to minimize animal suffering.

### 2.2. Experimental design

#### 2.2.1. Preliminarily dose finding study

A dose finding study was performed based on the dose range report by others [4]. With doses at the level of 0, 500 or 800 ppm (as $MnCl_2{\cdot}4H_2O$) in the basal diet, dams ($n = 3$/dose) were treated from GD 10 to PND 21. As a result, pups exposed to 800 ppm exhibited a slightly decreased body weight, but dams showed no effects in body weight or food consumption (data not shown).

#### 2.2.2. Experiment 1

Based on the results of preliminarily dose finding study, high dose was set at 800 ppm. Dams were randomly divided into four groups including untreated controls. Eight dams per group were treated with 0 (untreated control), 32, 160 or 800 ppm (as $MnCl_2{\cdot}4H_2O$) in the CRF-1 basal diet from GD 10 to PND 21.

Body weight and food consumption of dams were measured throughout the experimental period. The culling and selection of offspring at necropsy are summarized in Table 1. On PND 4, the litters were culled randomly, leaving four male and four female offspring per dam. The offspring were weighed at 3- or 4-day intervals. On PND 21, 16 male and 16 female offspring (two males and two females per dam) per group were subjected to pre-pubertal necropsy for the immunohistochemistry and apoptotic cell detection (10 males and 10 females per group with at least one male and one female per dam), determination of Mn concentration in the brain and real-time reverse transcription polymerase chain reaction (RT-PCR) analysis (six males and six females per group).

The remaining animals were kept through PND 77 and their body weights and food consumption were measured weekly. All offspring consumed the CRF-1 basal diet and tap water *ad libitum* from PND 21 onwards. On PND 77, 16 male and 16 female offspring (two males and two females per dam) per group were subjected to terminal necropsy for immunohistochemistry and apoptotic cell detection (10 males and 10 females per group with at least one male and one female per dam) and determination of Mn concentrations in the brain (six males and six females per group).

At both PND 21 and PND 77, female samples were only preserved without subject to further analysis.

External differentiation on landmarks of physical development was examined with regard to pinna detachment on PND 4, eruption of lower incisor on PND 11 and 14, opening of eyelid on PND 14 and 17, opening of vagina on PND 35 and 42, and cleavage of the balanopreputial gland on PND 42 and 49.

At necropsies of offspring on PND 21 and 77, weights of the brain, liver, kidneys, testes and ovaries were measured. All animals used in the present study were sacrificed by exsanguination from the abdominal aorta under deep anesthesia with ether.

#### 2.2.3. Experiment 2

To evaluate the effects of developmental exposure to $MnCl_2{\cdot}4H_2O$ on the serum concentrations of thyroid related hormones, additional experiments were performed. Dams were randomly divided into three groups including untreated controls. Six dams per group were treated with Mn at 800 or 1600 ppm (as $MnCl_2{\cdot}4H_2O$) in the CRF-1 basal diet from GD 10 to PND 21. On PND 4, the litters were culled randomly, leaving four male and four female offspring per dam. On PND 21, all dams and 10 male offspring per group from six dams (one or two males per dam) were

Please cite this article in press as: Ohishi T, et al. Reversible aberration of neurogenesis affecting late-stage differentiation in the hippocampal dentate gyrus of rat offspring after maternal exposure to manganese chloride. Reprod Toxicol (2012), http://dx.doi.org/10.1016/j.reprotox.2012.04.009

subjected to laparotomy under ether anesthesia and blood samples were collected from the abdominal aorta for hormone analysis. Ten males from the remaining animals (one or two males per dam) were kept through PND 77 and subjected to blood sample collection for hormone analysis on PND 77. After blood sampling, all animals were sacrificed by exsanguination from the abdominal aorta under deep anesthesia with ether.

### 2.3. Determination of Mn concentration in the brain

To measure Mn concentrations, the cerebellums of all dams and male and female offspring on PND 21 and 77 ($n = 6$/group for each stage) were removed, weighed, frozen in liquid nitrogen and stored at −80 °C until analysis. Samples of dams and male offspring were subjected to analysis (Table 1). Frozen cerebellar tissue was digested using a microwave oven (MARS5, CEM Corp., Matthews, NC, USA); the digested samples were analyzed using inductively coupled plasma mass spectrometer (ICP-MS, HP-7500; Hewlett-Packard Co., Palo Alto, CA, USA) with the monitoring mass of $m/z$ as 55 for Mn.

### 2.4. Hormone analysis

Blood samples were collected from the abdominal aorta under anesthesia. Serum was prepared and stored at −80 °C. Thyroid-stimulating hormone (TSH), triiodothyronine ($T_3$) and thyroxine ($T_4$) concentrations were measured by the chemiluminescent enzyme immunoassay method with the use of DPC IMMULYZE (Siemens Healthcare Diagnostics Inc., IL, USA).

### 2.5. Behavioral examinations

During the lactation period, sensory and reflex functional examination was conducted for two male and two female offspring in each litter. After weaning, detailed clinical observations, manipulative testing, measurement of grip strength, measurement of motor activity and water-filled multiple T-maze tests were conducted for one male and one female offspring in each litter. The method of each examination is described as follows.

#### 2.5.1. Sensory and reflex functional examinations

Surface righting reflex was examined on PND 10 and was measured as the time required to return to a normal position. Air righting reflex was examined on PND 15 and pupillary reflex, Preyer's reflex and pain reflex were examined on PND 21. The air righting reflex was assessed to examine the normal landing response of an animal to right itself from an inverted position in free fall of about 300 mm height. The pupillary reflex was assessed to examine the normal miotic response to the light. The Preyer's reflex was assessed to examine the normal pinna or startle response to the sound of the Galton's whistle. The pain reflex was assessed to examine the normal response such as avoiding and vocalization to the pinching stimuli of the tail.

#### 2.5.2. Detailed clinical observations

Detailed clinical observations were conducted on PND 29, 43 and 71. In home cage observations, animals were observed for posture, convulsion and abnormal behavior. During handling, animals were observed for ease of removal from cage, fur condition, skin, secretions of the eyes and nose, exophthalmos, palpebral closure, visible mucosal membranes, autonomic nervous functions (lacrimation, piloerection, pupil size, salivation, abnormal respiration), and vocalization and reactivity to handling.

#### 2.5.3. Manipulative testing

Following the detailed clinical observations on PND 71, animals were examined for auditory response, visual approach response, touch response, tail pinch response, pupillary reflex (light reflex), air righting reflex and measured landing foot splay (hind foot).

The auditory response was assessed to examine the normal startle response to clackety-clack stimuli. The visual approach response was assessed to examine the normal response such as sniffing or avoiding to the pen approaching the nose. The touch response was assessed to examine the normal response such as avoiding or soft vocalization to the pen touching the abdomen. The tail pinch response was assessed to examine the normal response such as quick avoiding and vocalization. The pupillary reflex and air righting reflex were assessed as mentioned above.

#### 2.5.4. Grip strength

Following the manipulative testing on PND 71, grip strengths of the forelimbs and hind limbs were measured using a CPU gauge MODEL-RX-5 (Aikoh Engineering Co., Ltd., Osaka, Japan).

#### 2.5.5. Motor activity

Following the measurement of grip strength on PND 71, motor activity was measured using an experimental animal motor activity sensor NS-AS01 (NeuroScience Inc., Tokyo, Japan). The length of measurement was 1 h. Values of 10-min intervals and the 0–60-min value were recorded.

#### 2.5.6. Water-filled multiple T-maze testing

To assess the learning ability, examination in water-filled multiple T-maze (Biel's type) as shown in Supplementary Fig. 1 [19,20] was performed from PND 55 to 57. In this test, animals were subjected to a series of right/left choices to get from one end of the water-filled maze to find the escape. Elapsed time to reach the goal and error counts (number of times the whole body entered into the error area) were measured in three trials each day. The interval of each trial was approximately 5–10 min. The maximum elapsed time for each trial was set at 3 min, and the trials where animals did not reach the goal within 3 min were excluded from statistical analysis. On the 1st day, 1 male in the untreated controls and 1 male in the 160 ppm group at the 1st trial, 1 female in the untreated controls and 1 female in the 800 ppm group at the 2nd trial and 1 female in the untreated controls in the 3rd trial did not reach the goal; however, there were no differences in the number of unreached animals between the untreated controls and any of the treatment groups. Unreached animal data were excluded from the analysis.

One day before the initiation of T-maze test, animals were subjected to examination of swimming ability using a straight course as shown in Supplementary Fig. 1. Elapsed time required to reach the goal was recorded in three trials. There were no differences in the elapsed time using the straight course in both sexes at all doses, indicating no effects on swimming ability (Supplementary Table 1).

### 2.6. Immunohistochemistry and apoptotic cell detection

The brains of the male offspring sacrificed at PND 21 and 77 were fixed in Bouin's solution at room temperature overnight. Ten male animals from eight dams (one or two males per dam) per group were subjected to analysis at each time point. Coronal slices at the positions of −3.0 and −3.5 mm from the bregma were prepared from the PND 21 and 77 brains, respectively. Brains were routinely processed by paraffin embedding and sectioned at 3 μm.

For immunohistochemistry studies, the brain sections were incubated at 4 °C overnight with antibodies against doublecortin (DCX, rabbit IgG, 1:1000, Abcam, Cambridge, UK), a microtubule binding protein that is expressed in the type-2b and type-3 progenitor cells and immature neurons [11]; T box brain 2 (Tbr2, rabbit IgG, 1:500, Abcam, Cambridge, UK), a transcription factor that is expressed in the type-2 progenitor cells [21]; glial fibrillary acidic protein (GFAP, clone GA5, mouse $IgG_1$, 1:200, Millipore Corporation, Temecula, CA, USA), an intermediate filament that is expressed not only in astrocytes but also type-1 progenitor cells [11]; reelin (clone G10, mouse $IgG_1$, 1:1000; Novus Biologicals, Inc., Littleton, CO, USA), a secreted extracellular matrix glycoprotein that plays a critical role in neuronal migration and positioning during brain development [13]; neuron-specific nuclear protein (NeuN; clone A60, mouse $IgG_1$, 1:100, Millipore Corporation, Temecula, CA, USA), which specifically detects post-mitotic neurons [22]; glutamic acid decarboxylase 67 (GAD67; clone 1G10.2, mouse $IgG_{2a}$, 1:50, Millipore Corporation), a GABA-synthesizing enzyme that is expressed in GABAergic neurons [23]; and proliferating cell nuclear antigen (PCNA; clone PC10, mouse $IgG_{2a}$, 1:200, Dako, Glostrup, Denmark). To quench endogenous peroxidase, the slides were incubated in 0.3% hydrogen peroxide in absolute methanol for 30 min. Immunodetection was carried out using a VECTASTAIN® Elite ABC kit (Vector Laboratories Inc., Burlingame, CA, USA) with 3,3′-diaminobenzidine/$H_2O_2$ as the chromogen, as previously described [24]. The sections were then counterstained with hematoxylin and coverslipped for microscopic examination.

For evaluation of apoptosis in the SGZ of the dentate gyrus, a terminal deoxynucleotidyl transferase dUTP nick end labeling (TUNEL) assay was applied to brain sections. Deparaffinized sections were treated with 20 μg/mL of proteinase K in phosphate buffered saline (PBS; pH 7.4) for 15 min at room temperature, and then incubated in 3.0% hydrogen peroxide in PBS for 5 min. Detection of apoptotic cells was carried out using the Apop Tag® *in situ* apoptosis detection kit (Millipore Corporation) according to the instructions provided by the manufacturer with 3,3′-diaminobenzidine/$H_2O_2$ as the chromogen. The same 10 male offspring from eight dams (one or two males per dam) per group at each time point were used for all immunohistochemical studies and the TUNEL assay.

### 2.7. Morphometry of immunolocalized and apoptotic cells

The SGZ in the dentate gyrus is known for its neurogenesis during development and throughout the postnatal life of granule cells [10,11]. Therefore, DCX-, Tbr2- or GFAP-positive cells as those consisting of granule cell lineage, apoptotic cells as detected by the TUNEL method and proliferating cells as detected by nuclear immunoreactivity of PCNA were bilaterally counted in the SGZ and normalized for the length of the granule cell layer measured as previously described (Fig. 1) [7]. In the hilus of the dentate gyrus, GABAergic interneurons, especially reelin-synthesizing ones, are known to modulate migration and correct positioning of progenitor granule cells [17]. Therefore, reelin- or GAD67-immunoreactive interneurons distributed in the hilus were bilaterally counted and normalized for the number per area unit of the hilar area (polymorphic layer) as previously described (Fig. 1) [7]. We also measured NeuN-positive neurons in the hilus as those of postmitotic interneurons fluctuating in the number in response to aberrant neurogenesis or neuronal mismigration [7]. Large-sized CA3 neurons distributed in this area were easily distinguished from hilar interneurons and excluded from counting as previously described (Fig. 1) [7]. For quantitative measurement of each immunoreactive

Please cite this article in press as: Ohishi T, et al. Reversible aberration of neurogenesis affecting late-stage differentiation in the hippocampal dentate gyrus of rat offspring after maternal exposure to manganese chloride. Reprod Toxicol (2012), http://dx.doi.org/10.1016/j.reprotox.2012.04.009